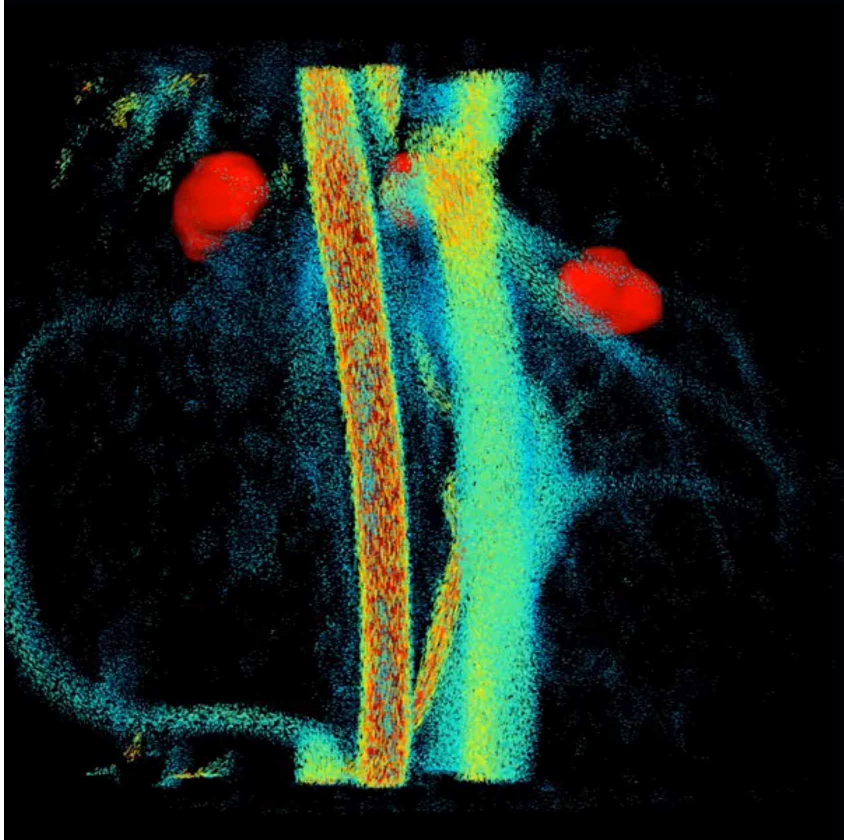

Improving Precision of Image-Guided Cancer Therapy with MRI guidance

Jason Chiang, MD, PhD

Assistant Professor

Division of Interventional Radiology

Department of Radiological Sciences

UCLA Ronald Reagan Medical Center, Los Angeles, CA

Disclosures

- J.C. receives licensing fees for patents relating to MWA through the Wisconsin Alumni Research Foundation; equipment support from Ethicon Neuwave Medical Inc.

Global Burden of HCC

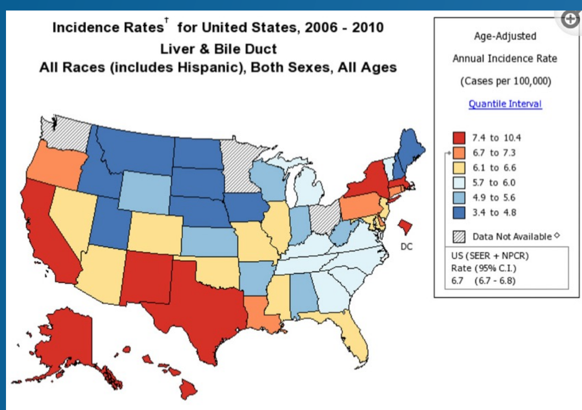

- Hepatocellular carcinoma is one of the most common form of liver cancer with an estimated case incidence of >1 million by 2025
- Rates have tripled in the United States over the last 3 decades
- Hepatitis B and C are the main risk factors for HCC development, although NASH is becoming a bigger risk factor in the West.
- Asians and Hispanics have the highest incidence rates of HCC in the United States -> 1/3 live in CA.

~40/100,000 in CA alone

Llovet JM et al. Hepatocellular carcinoma. Nat Rev Dis Primers. 2021 Jan 21;7(1):6.
Han SS et al. . Changing Landscape of Liver Cancer in California: A Glimpse Into the Future of Liver Cancer in the United States. J Natl Cancer Inst. 2019 Jun 1;111(6):550-556.

Diagnosing HCC

Diagnosis, Staging, and Management of Hepatocellular Carcinoma: 2018 Practice Guidance by the American Association for the Study of Liver Diseases

Jorge A. Marrero,[1] Laura M. Kulik,[2] Claude B. Sirlin,[3] Andrew X. Zhu,[4] Richard S. Finn,[5] Michael M. Abecassis,[2] Lewis R. Roberts,[6] and Julie K. Heimbach[6]

→

Diagnosis

2. The AASLD recommends diagnostic evaluation for HCC with either multiphase CT or multiphase MRI because of similar diagnostic performance characteristics.

Quality/Certainty of Evidence: Low for CT versus MRI

Strength of Recommendation: Strong

LR-1	Definitely benign
LR-2	Probably benign
LR-3	Intermediate probability of malignancy
LR-4	Probably HCC
LR-5	Definitely HCC
LR-M	

CT/MRI Diagnostic Table

Arterial phase hyperenhancement (APHE)		No APHE		Nonrim APHE		
Observation size (mm)		< 20	≥ 20	< 10	10-19	≥ 20
Count additional major features: • Enhancing "capsule" • Nonperipheral "washout" • Threshold growth	None	LR-3	LR-3	LR-3	LR-3	LR-4
	One	LR-3	LR-4	LR-4	LR-4 / LR-5	LR-5
	≥ Two	LR-4	LR-4	LR-4	LR-5	LR-5

LR-4 / LR-5: Observations in this cell are categorized based on one additional major feature:
- LR-4 – if enhancing "capsule"
- LR-5 – if nonperipheral "washout" **OR** threshold growth

BCLC guidelines

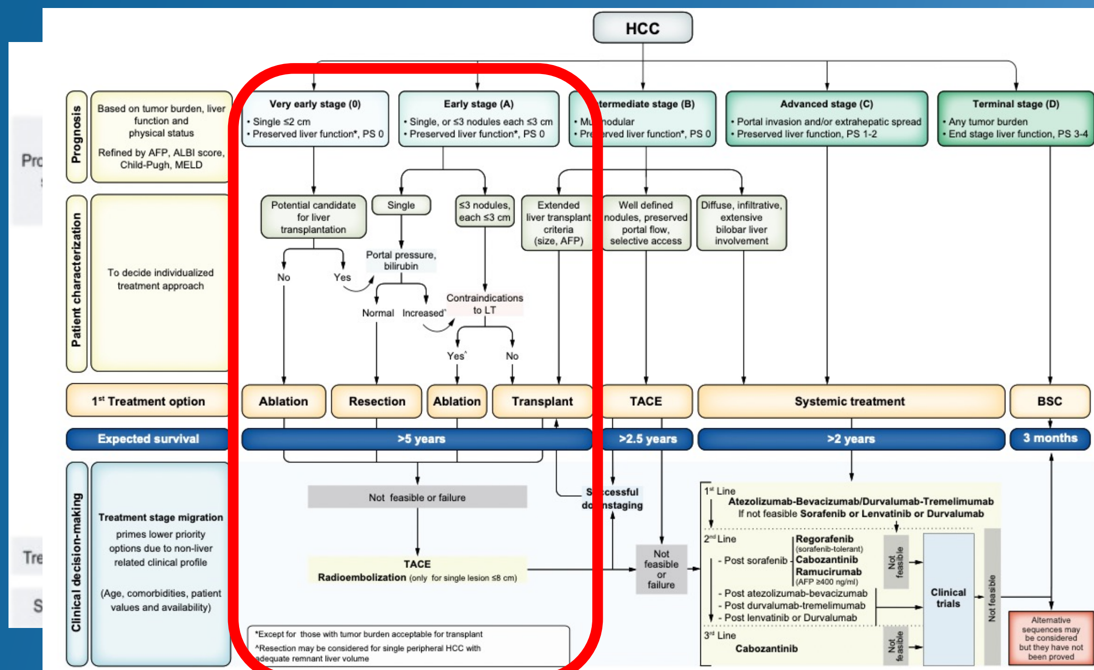

Reig M, Forner A, Rimola J, Ferrer-Fàbrega J, Burrel M, Garcia-Criado Á, Kelley RK, Galle PR, Mazzaferro V, Salem R, Sangro B, Singal AG, Vogel A, Fuster J, Ayuso C, Bruix J. BCLC strategy for prognosis prediction and treatment recommendation: The 2022 update. J Hepatol. 2022 Mar;76(3):681-693.

Cross Sectional Imaging: MRI Abdomen

Case Example: Diagnostic evaluation

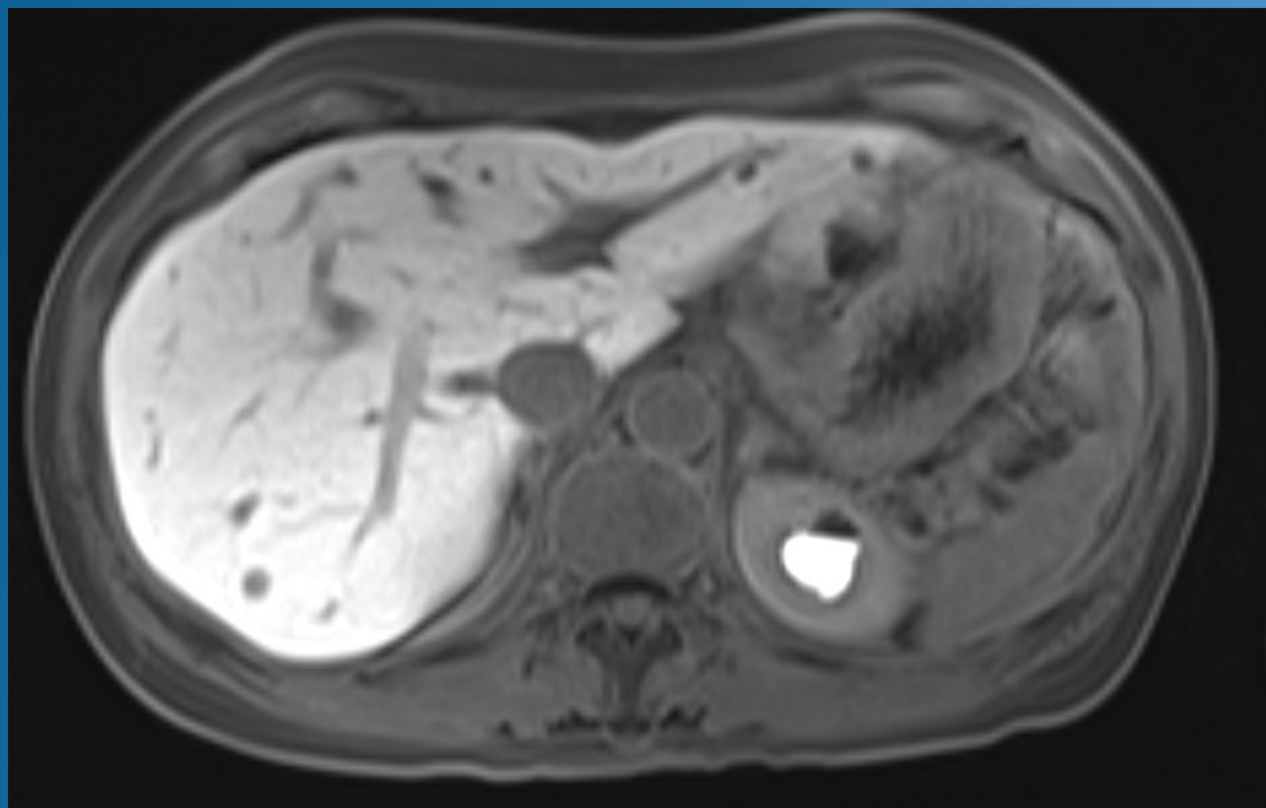

How do we do ablations?

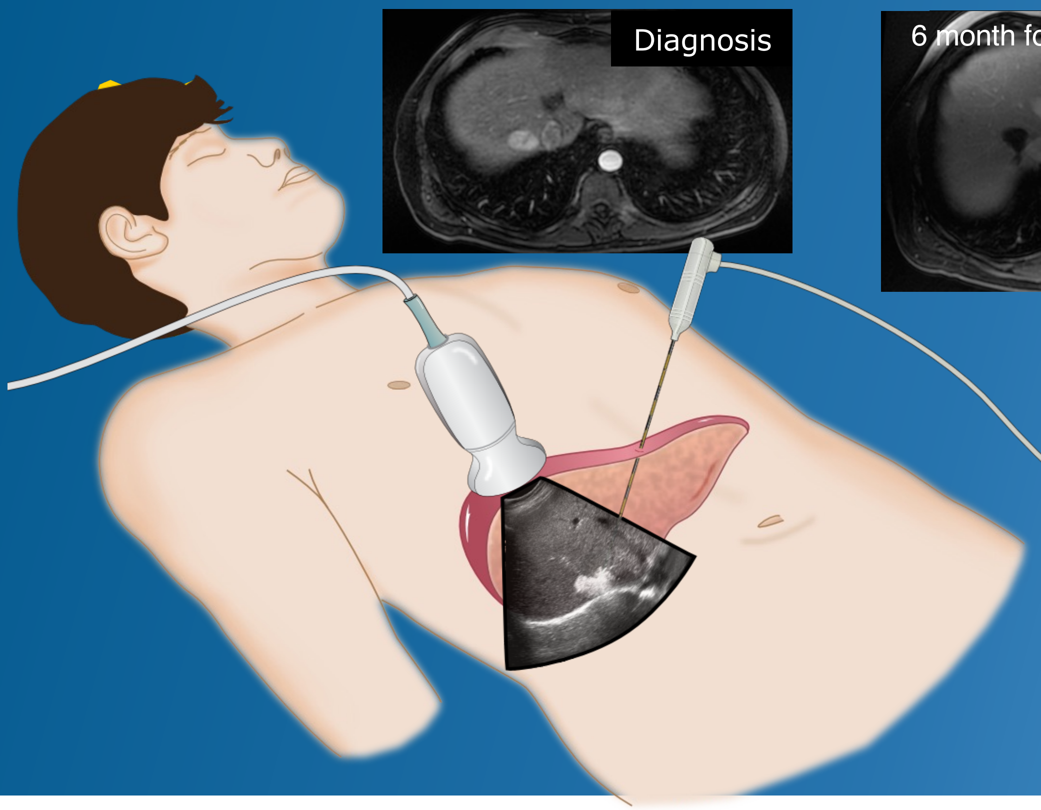

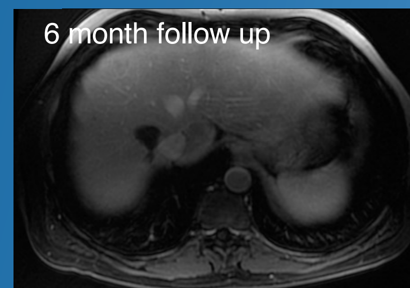

MWA vs RF: Differences in energy source

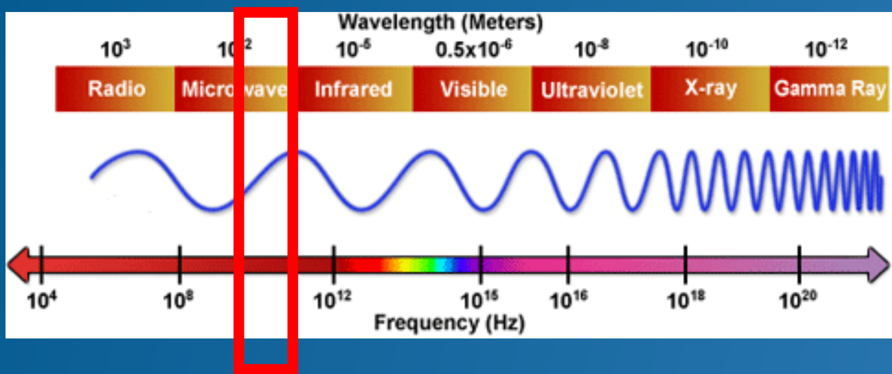

915 MHz
2.45 GHz

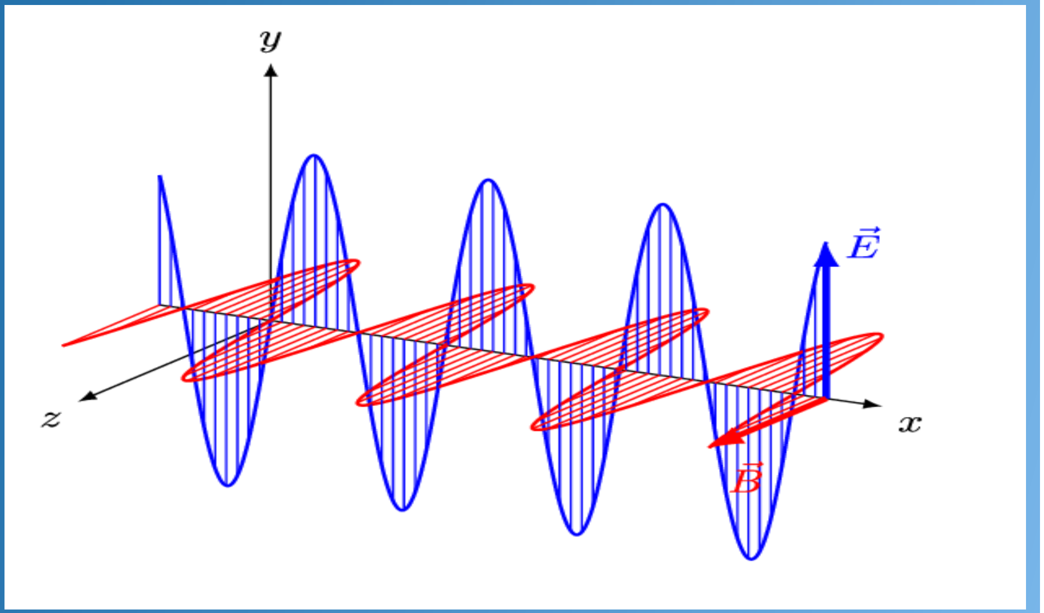

Ablation planning and treatment

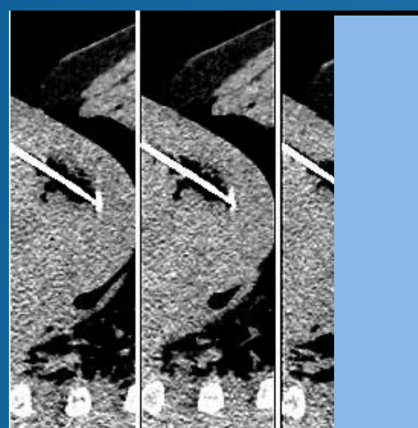

<u>Variables at play</u>:

- Tissue type
- Physiology
- Operator mechanics
- MWA antenna design

tumor size

visualize anatomy

visualize trajectory.

e manufacturer guidelines

Insufficient Heating

Technically successful ablation

Excess heating

Benefits of computational modeling

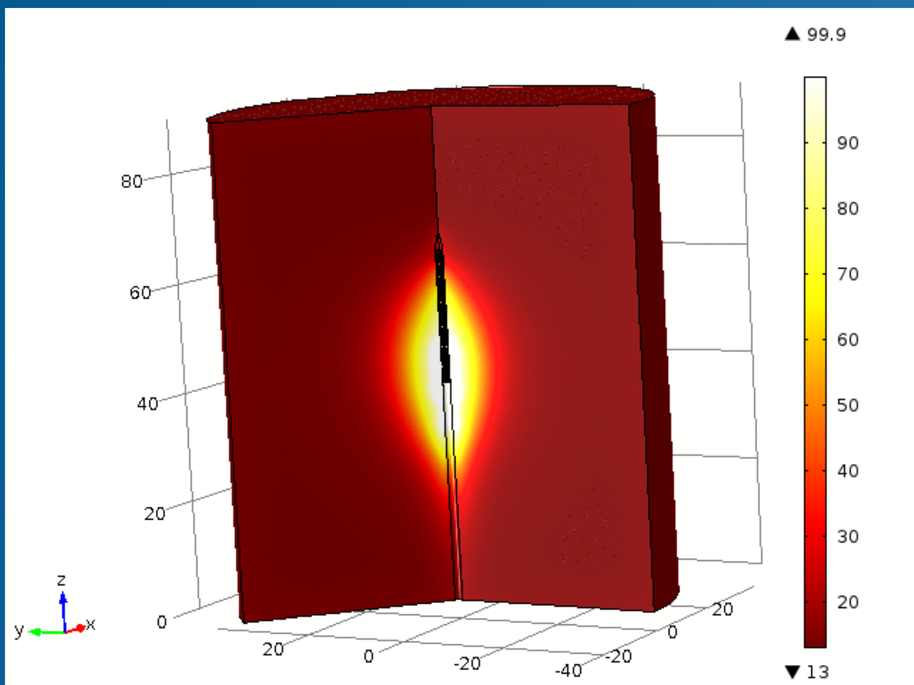

Create a highly controlled environment to investigate and understand the effects of changing individual input variables

- Laboratory Work
  - More focused experimental studies
  - Fewer animal studies
  - Decreased developmental costs
  - Greater research efficiency

- Clinical Work
  - Tailor treatment to patient-specific environments
  - Optimize device settings before a procedure

Margins are critical – use modeling to help you predict it ahead of time!

Margin	LTP rate
<= 5 mm	60% (21/35)
5-10 mm	10.5% (2/19)
>10 mm	0% (0/6)

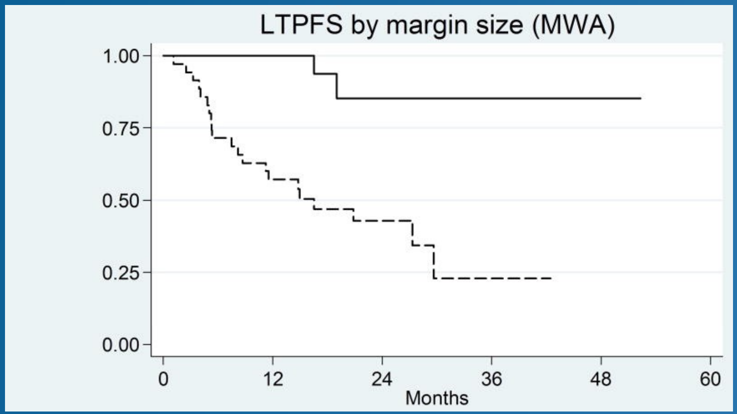

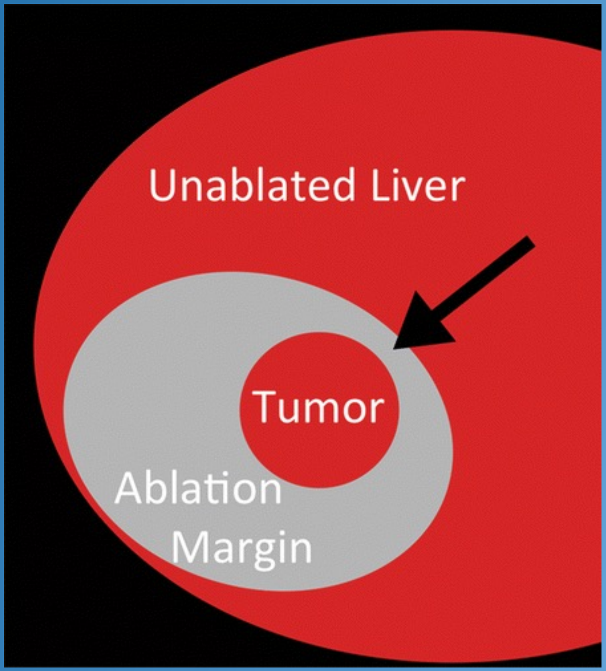

Shady, Waleed, Elena N. Petre, Kinh Gian Do, Mithat Gonen, Hooman Yarmohammadi, Karen T. Brown, Nancy E. Kemeny, et al. "Percutaneous Microwave versus Radiofrequency Ablation of Colorectal Liver Metastases: Ablation with Clear Margins (A0) Provides the Best Local Tumor Control." *Journal of Vascular and Interventional Radiology* 29, no. 2 (February 2018): 268-275.e1.

Modeling ablations: Basics in heat transfer

Ablation Modality	Max temperature	Mechanism of Heating	Risk:
Radiofrequency Ablation	<100 ℃	**Thermal Conduction**	Insufficient heat, higher recurrence rate

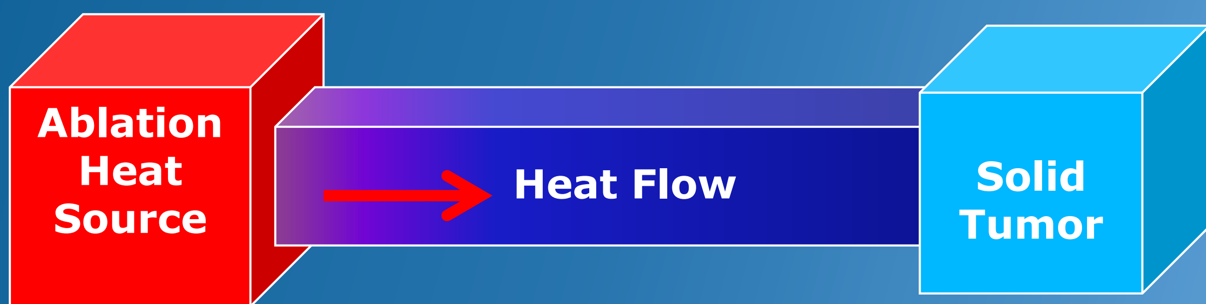

$$P_{conduction} = \frac{Q}{t} = kA\frac{T_h - Tc}{L}$$

Modeling MWA: Mechanism of heating

Ablation Modality	Max temperature	Mechanism of Heating	Risk:
Microwave Ablation	>100 ℃	**Thermal Conduction + Active Heating + Water Vapor**	Inadvertent damage, thrombosis

Factors that make MWA amenable to modeling

- **Tissue-specific heating** based on antenna design
- Less susceptibility to the heat-sink effect

Laeseke et al *JVIR* 20:1224-1229, 2009.

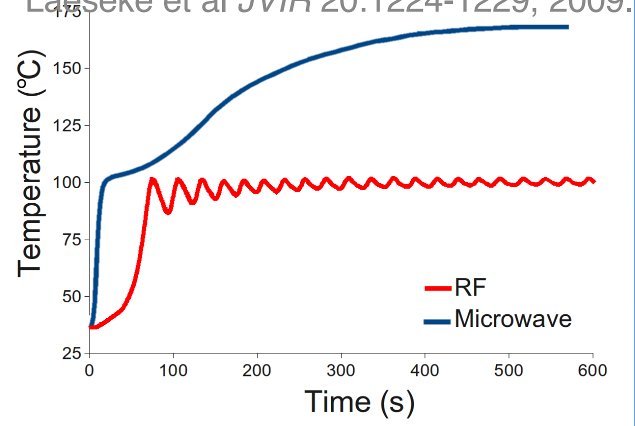

Basic computational setup and output

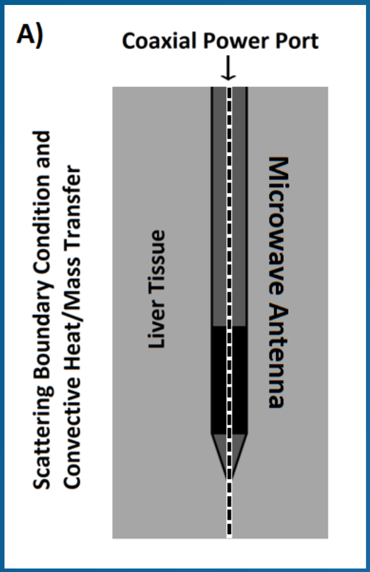

Specify the environment and antenna geometry

1) Solve Maxwell's equation to get time-dependent electromagnetic field propagation

$\nabla \cdot \mathbf{D} = \rho$	(1)	Gauss' Law
$\nabla \cdot \mathbf{B} = 0$	(2)	Gauss' Law for magnetism
$\nabla \times \mathbf{E} = -\frac{\partial \mathbf{B}}{\partial t}$	(3)	Faraday's Law
$\nabla \times \mathbf{H} = \frac{\partial \mathbf{D}}{\partial t} + \mathbf{J}$	(4)	Ampère-Maxwell Law

2) Solve for heat generation from electric field vector

$$Q = \frac{1}{2}\sigma|E|^2 \quad (W/m^3)$$

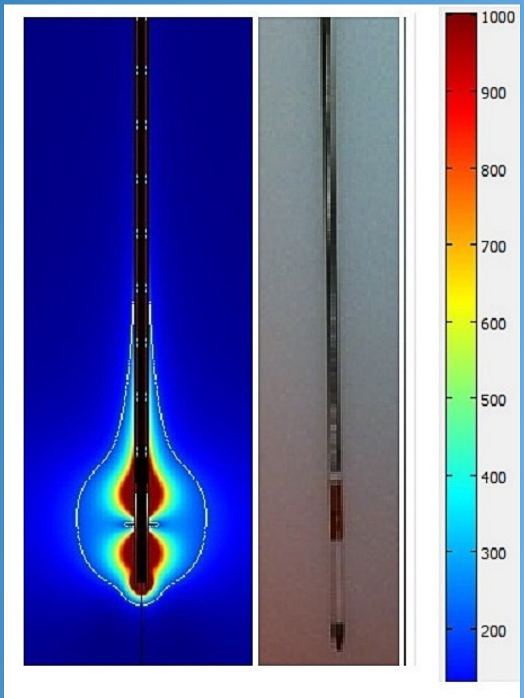

Chiang J, Wang P, Brace CL. Computational modelling of microwave tumor ablations. *Int J Hyperthermia*. 2013;29(4):308–317.

Tool Optimization: Organ-specific design

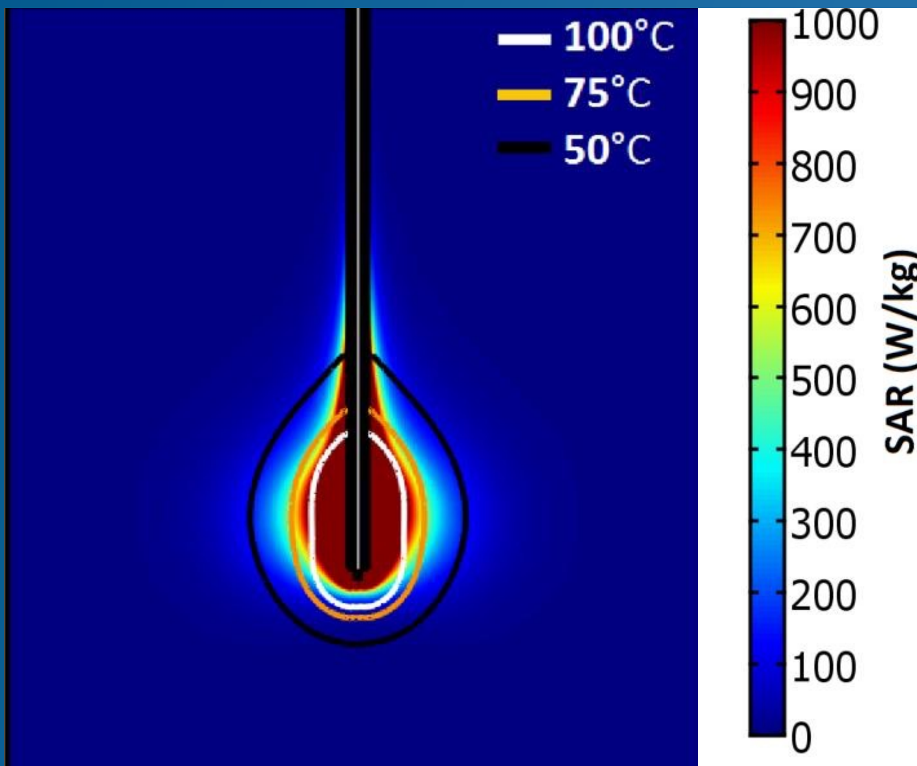

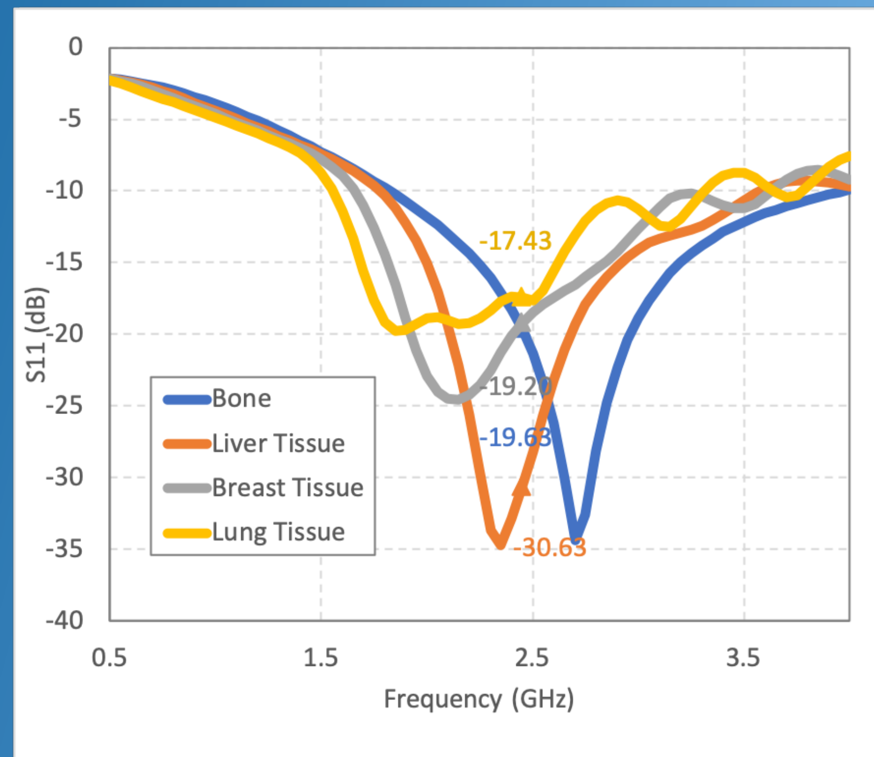

Tool Optimization: Shape-specific design

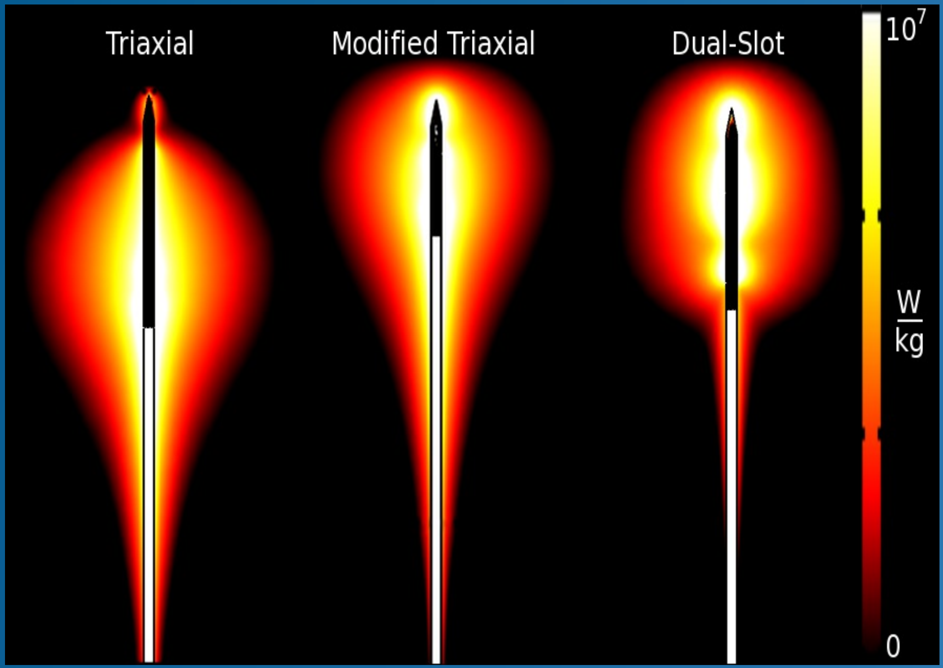

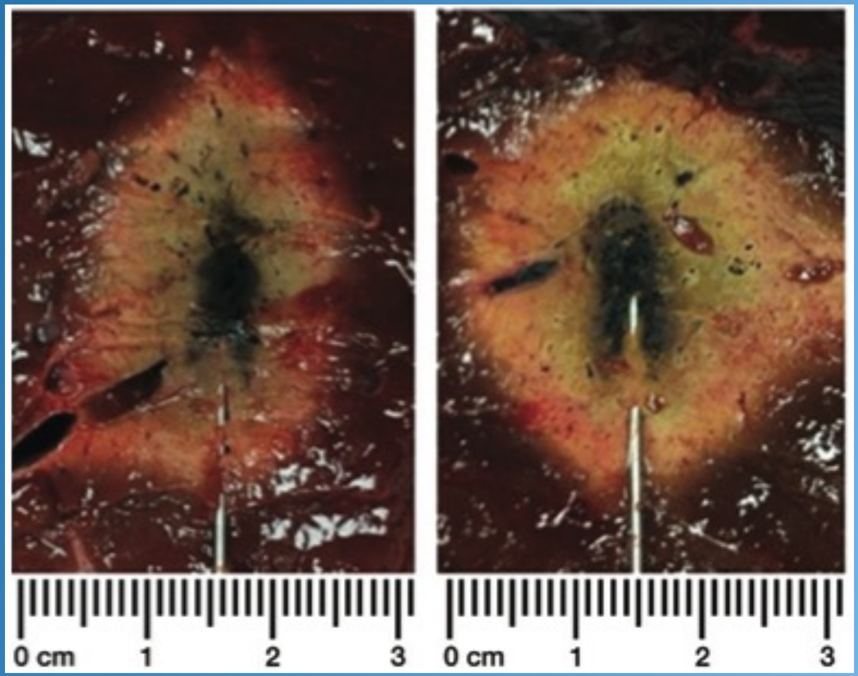

Chiang et al. *Radiology* 268:382-89, 2013.

Comparison between lung-tuned and liver-tuned antennas

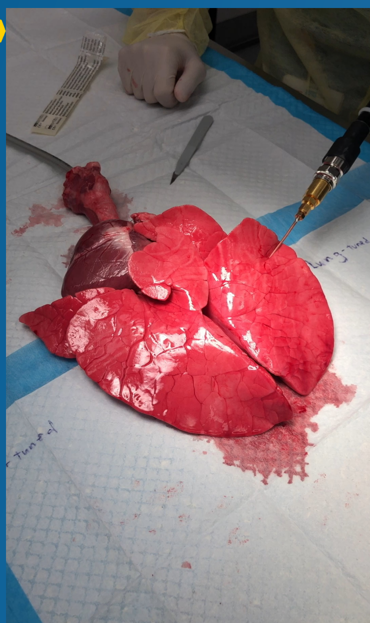

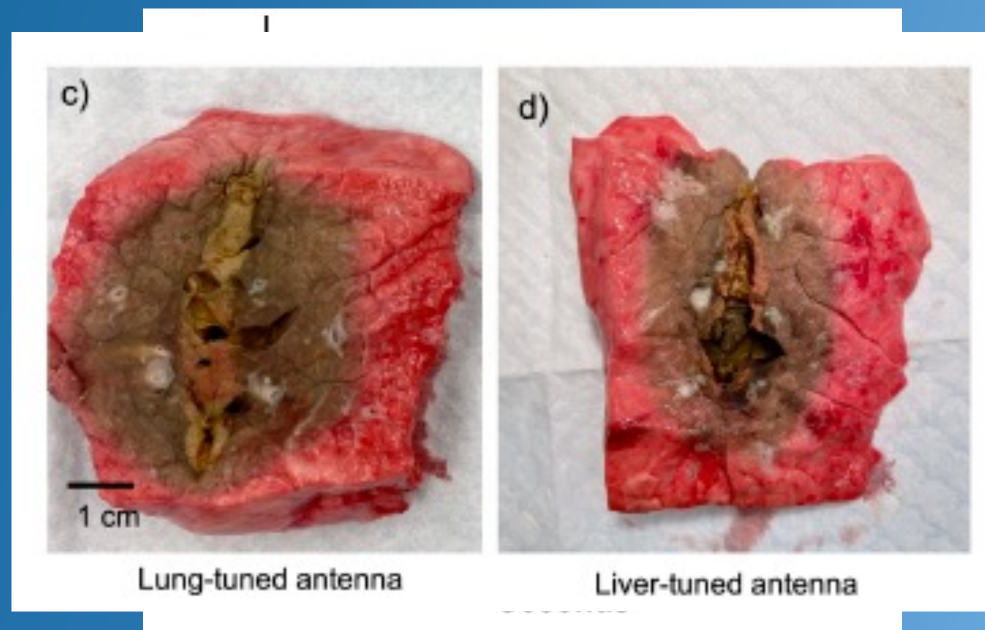

J. Chiang, L. Song, F. Abtin and Y. Rahmat-Samii, "Efficacy of Lung-Tuned Monopole Antenna for Microwave Ablations: Analytical Solution and Validation in a Ventilator-Controlled ex-vivo Porcine Lung Model," in *IEEE Journal of Electromagnetics, RF and Microwaves in Medicine and Biology (in press)*

Tunable Microwave Antennas

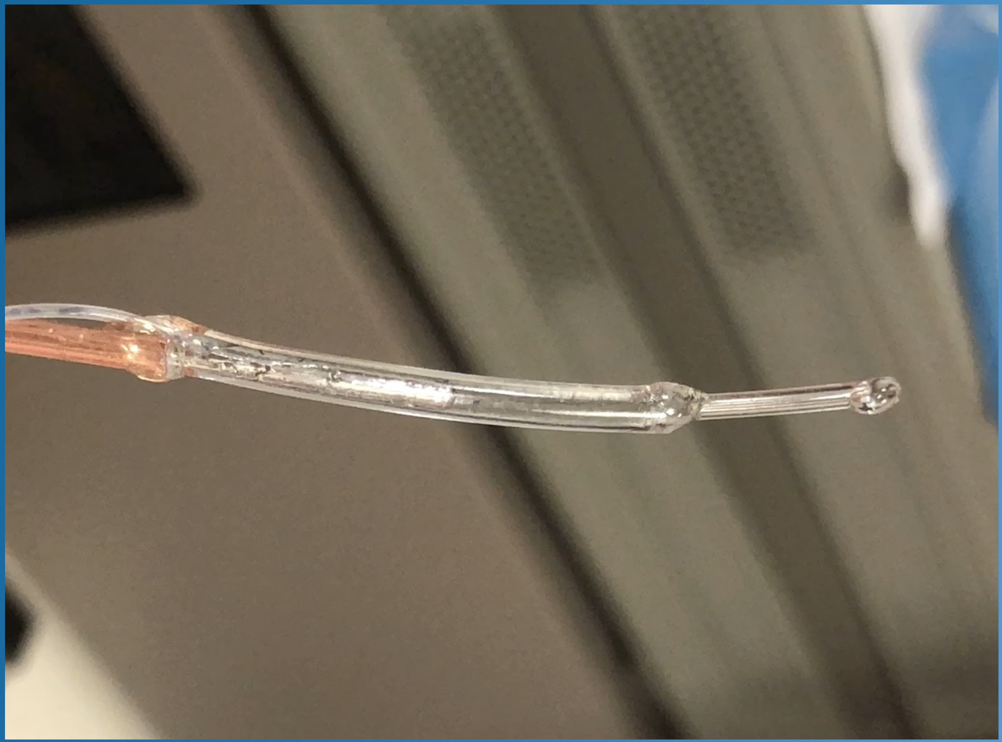

Thermal ablations and the heat-sink effect

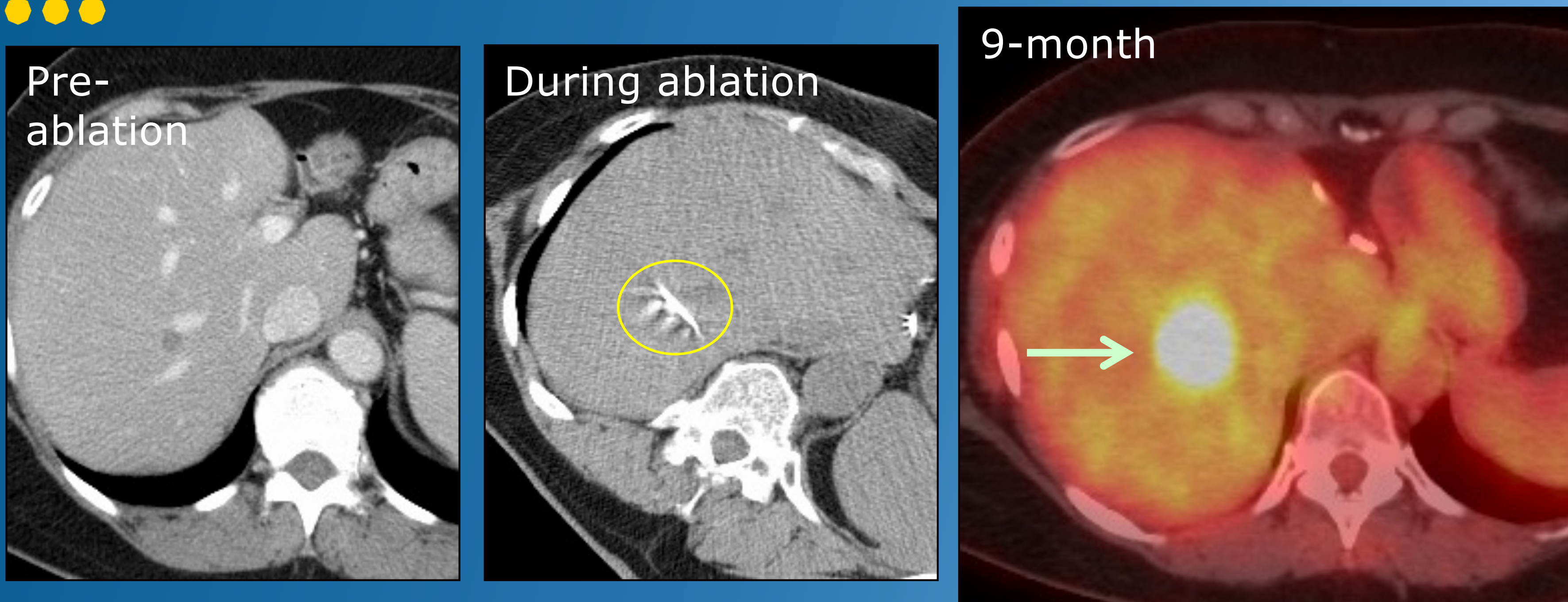

Calculating time-dependent temperature maps

Continuum approach: Use Pennes bioheat equation to create time-dependent ablation isotherms:

$$\nabla \cdot k \nabla T - \rho_b c_b \omega_b (T_{a0} - T) + q_m + Q = \rho c \frac{\partial T}{\partial t}$$

Thermal conduction — Blood flow — Metabolic heat — Heat source

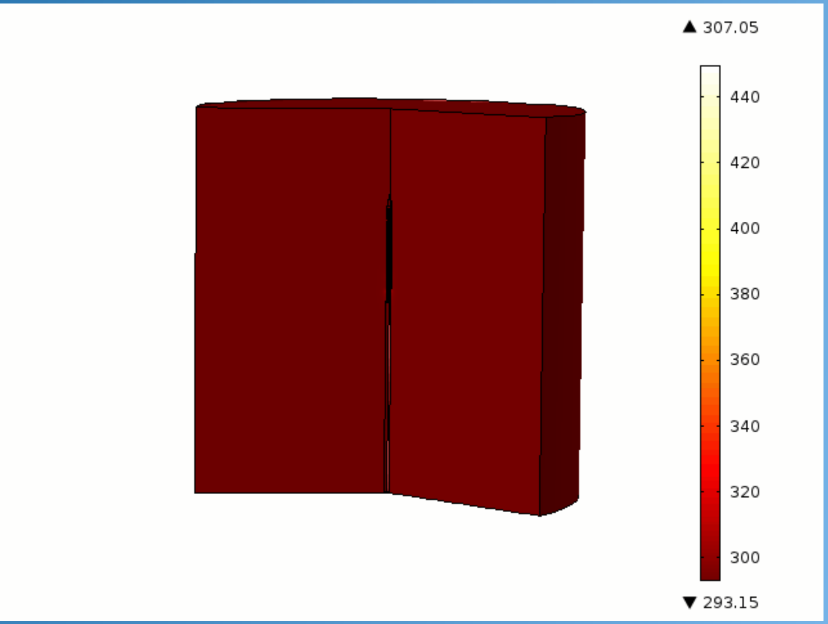

Calculating time-dependent temperature maps

Vascular approach: Model the impact of each vessel individually – mimic the *patient-specific* vascular anatomy for each ablation zone

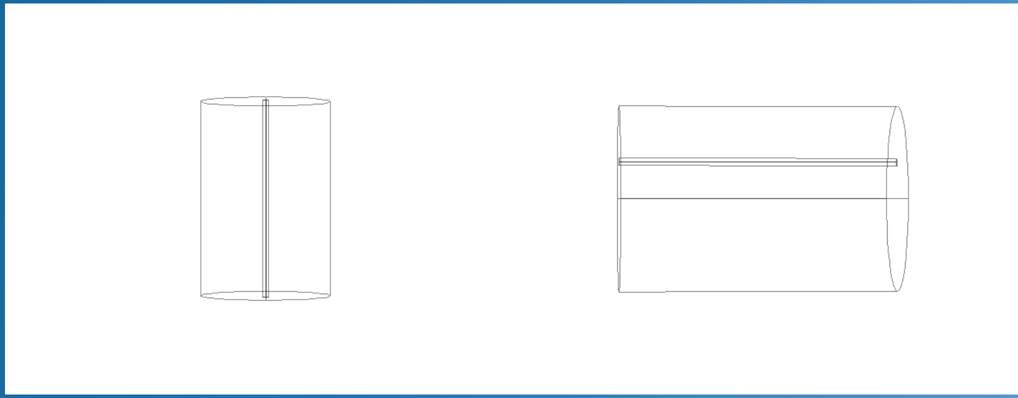

2D Phase Contrast

- One directional through-plane (Z) velocity encoding sequence
  - Acquisition of 2 images:
    - 1 Magnitude image
    - 1 Phase image

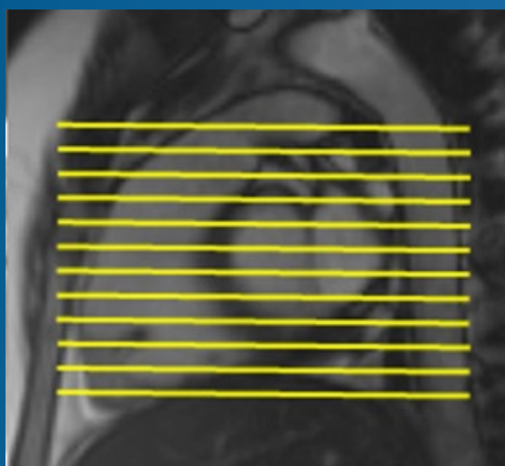

Region of Interest: Targeting vessel or anatomy

Magnitude image: Signal intensity proportional to velocity but no directional information

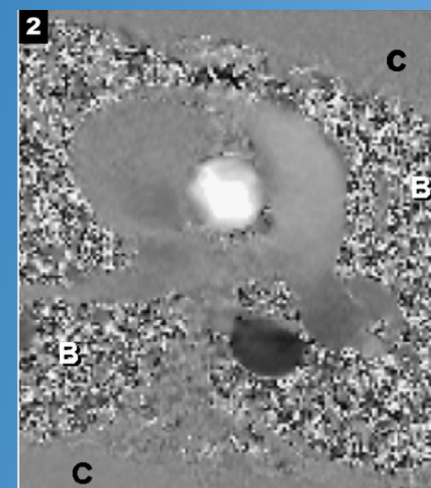

Phase image: blood flow shows directional information

4D flow MRI

- One directional through-plane (Z) velocity encoding sequence
  - Acquisition of 4 images: 1 Magnitude image + 3 Phase image

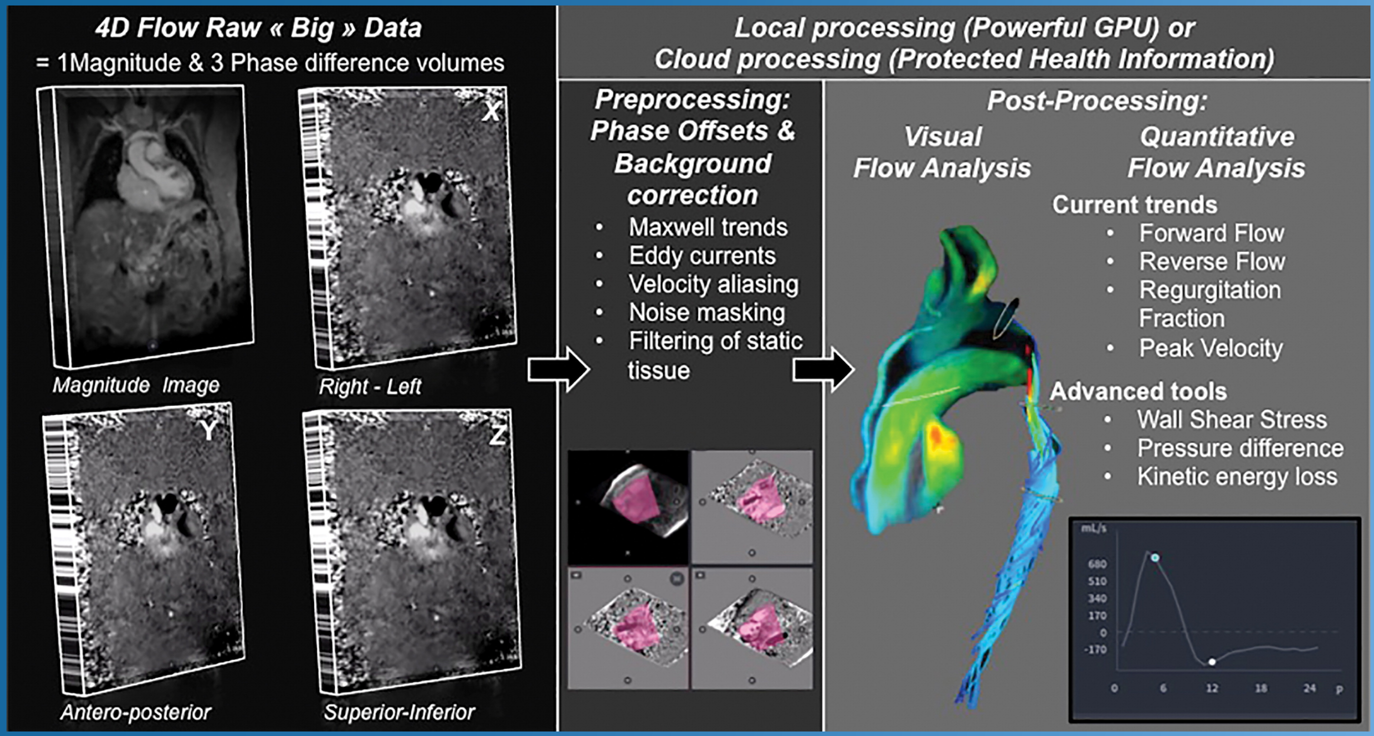

Azarine A, Garçon P, Stansal A, Canepa N, Angelopoulos G, Silvera S, Sidi D, Marteau V, Zins M. Four-dimensional Flow MRI: Principles and Cardiovascular Applications. Radiographics. 2019 May-Jun;39(3):632-648. doi: 10.1148/rg.2019180091. Epub 2019 Mar 22

4D flow MRI: Neuro applications

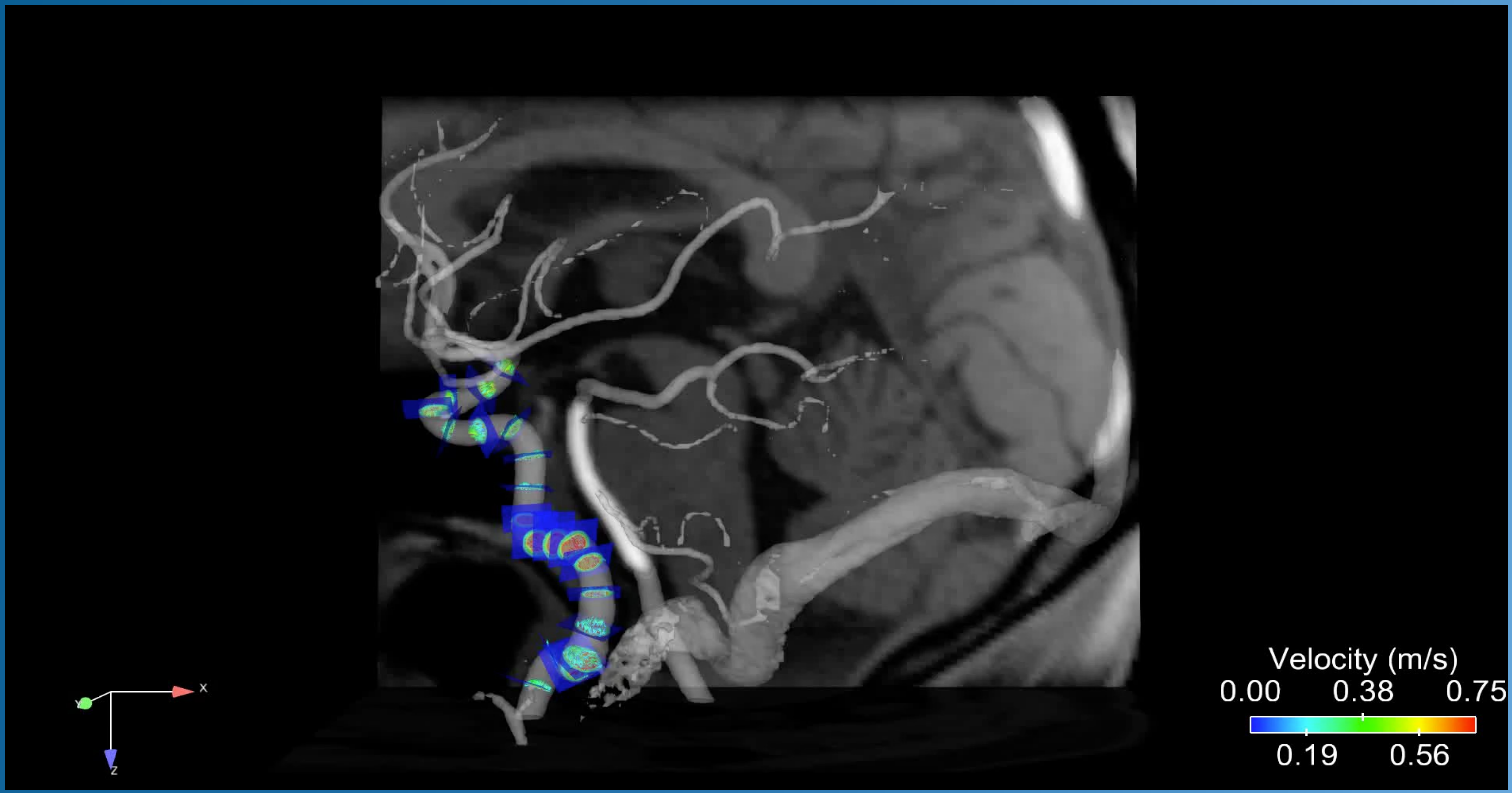

4D flow MRI: Visualizing Flow

Particle traces in the cardiac system

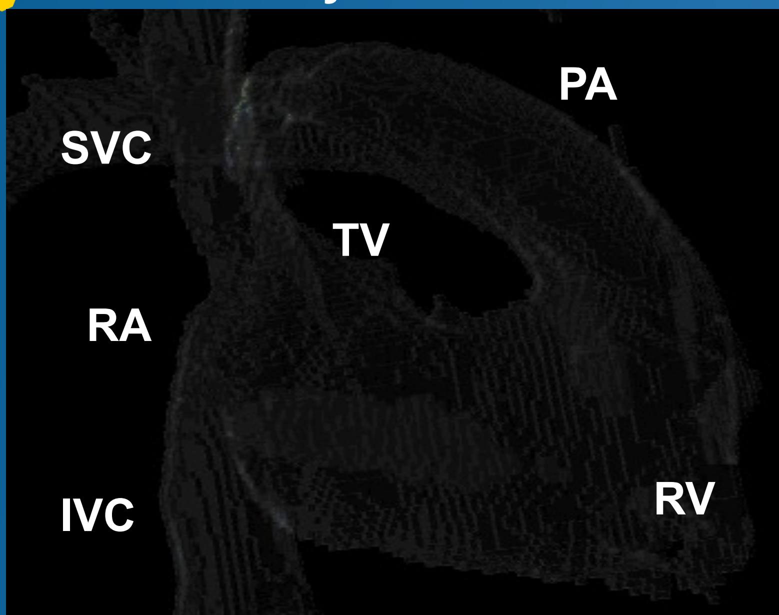

Streamlines in the Liver

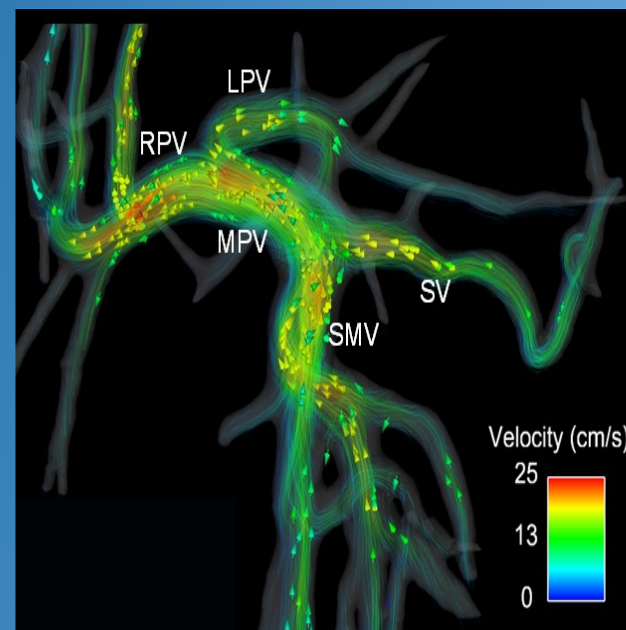

4D flow: Liver Applications

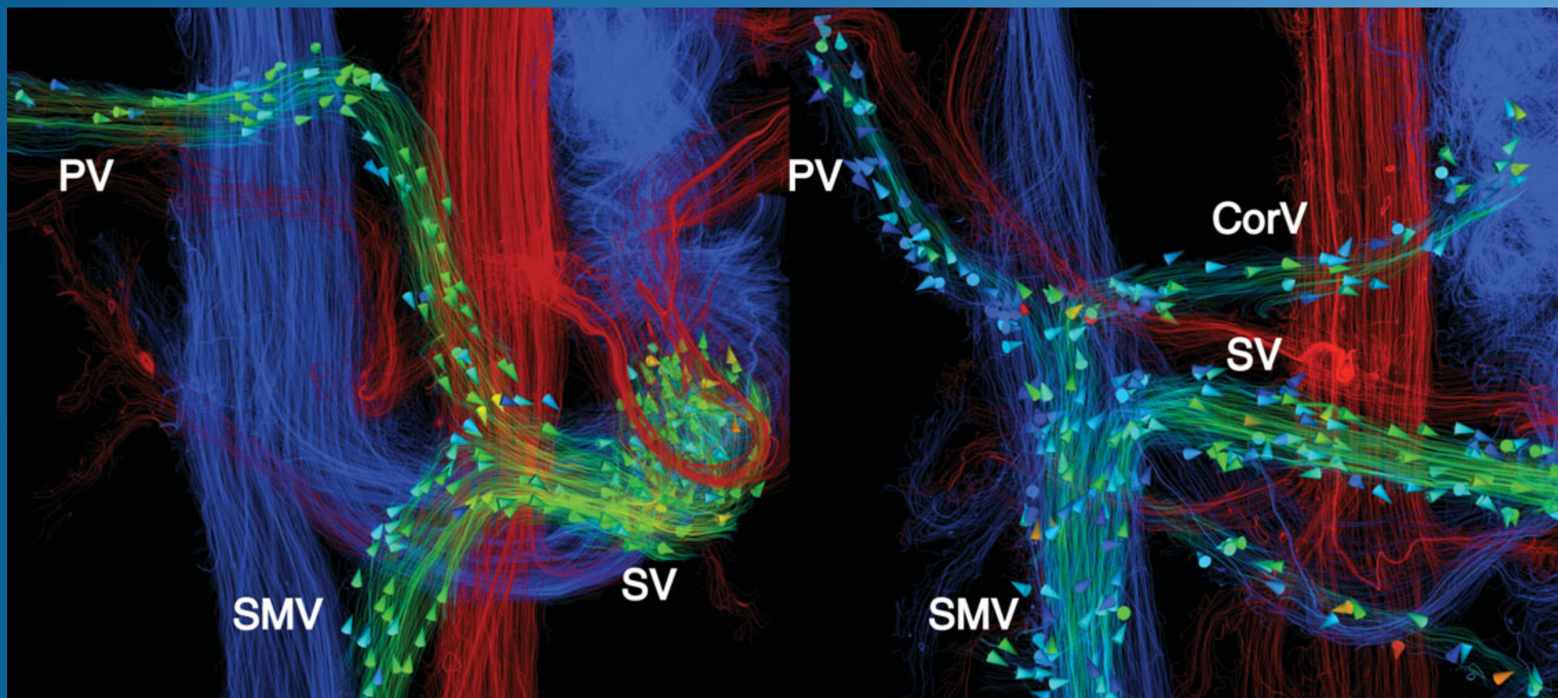

Physiological variation in blood flow through the portal vein due to the increased resistance in two patients with **portal hypertension.** a: Reversed (hepatofugal) flow is seen in the portal and splenic veins. Conservation of mass analysis showed good agreement (4.57%) between QPV and QSMV þ QSV. b: Reversed QSV with reduced QPV and normal QSMV.

Hepatic Angiogram showing similar reversal of flow

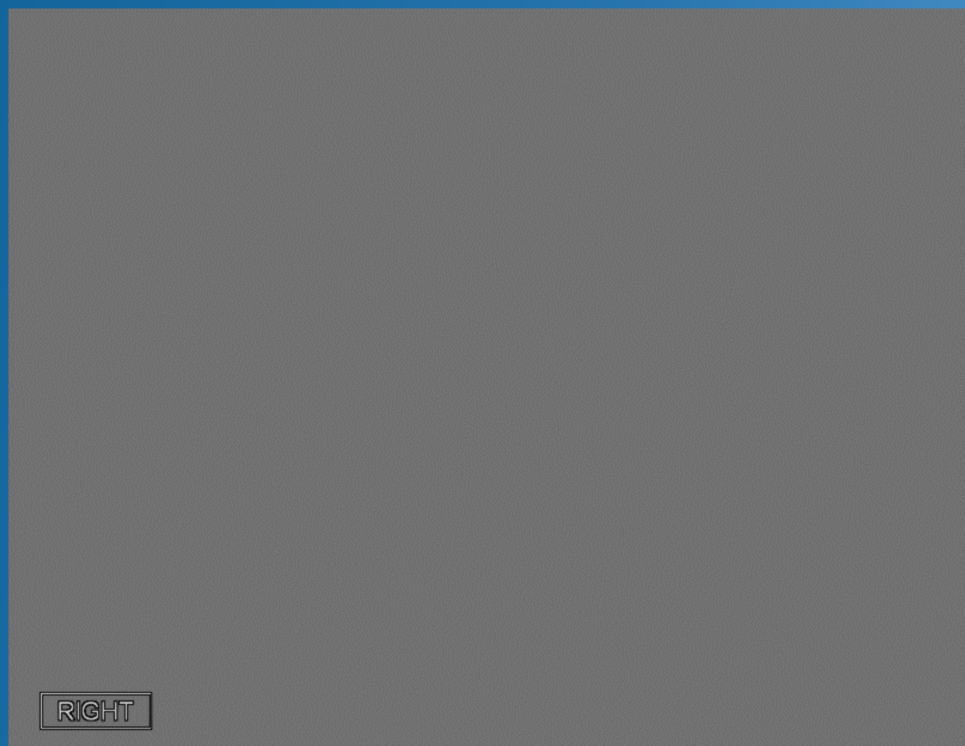

4D flow: Liver Applications

Four-dimensional–flow MR imaging– based visualization and quantification of hemodynamics in the portal system **before and after TIPS placement** in a 54-year-old man with portal hypertension and refractory ascites.

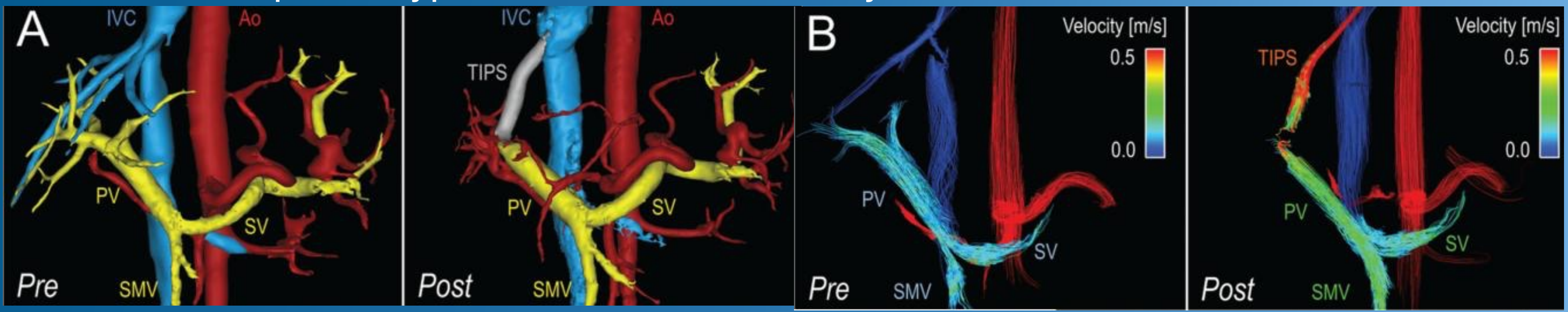

A) Segmentation of 4D-flow angiograms obtained before (pre) and 2 weeks after (post) TIPS placement show arteries (red), veins (blue), portal vasculature (yellow), and TIPS (gray).

B) Velocity-coded 4D-flow MR images obtained before and 2 weeks after TIPS placement show velocity distribution in the portal circulation. Note the high velocity in the TIPS, with a signal dropout at the proximal end of the TIPS due to disordered flow.

Roldán-Alzate, Alejandro, Christopher J. Francois, Oliver Wieben, and Scott B. Reeder. “Emerging Applications of Abdominal 4D Flow MRI.” *AJR. American Journal of Roentgenology* 207, no. 1 (July 2016): 58–66.

4D flow: Ablation-related hemodynamics

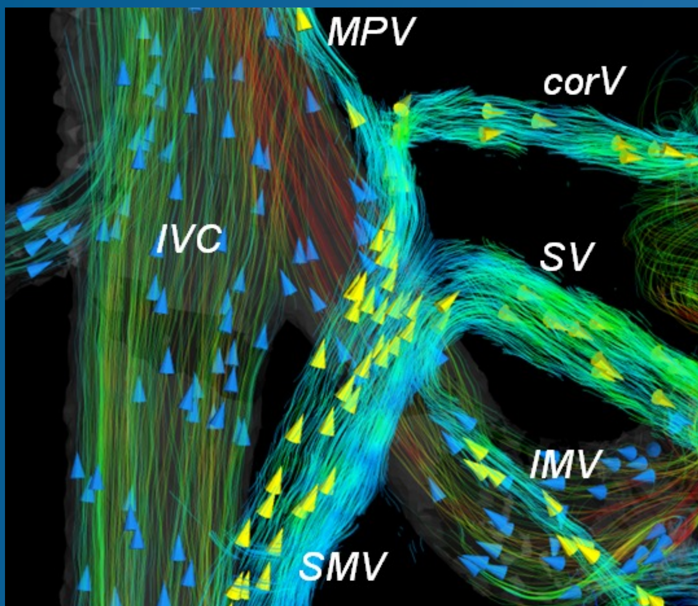

4D Flow images showing flow within the portal veins and IVC.

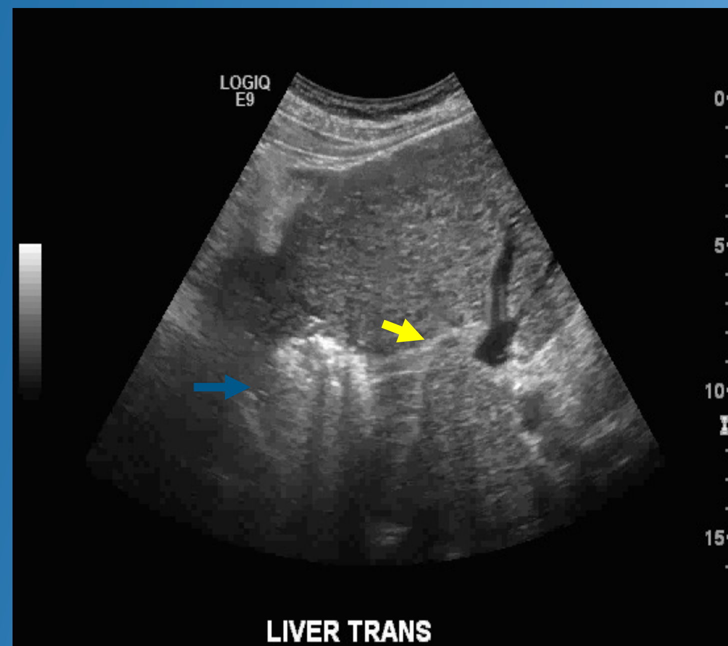

MWA zone (blue arrow) creating water vapor (yellow arrow) that is recondensing while in the hepatic vein.

4D flow: Ablation-related hemodynamics

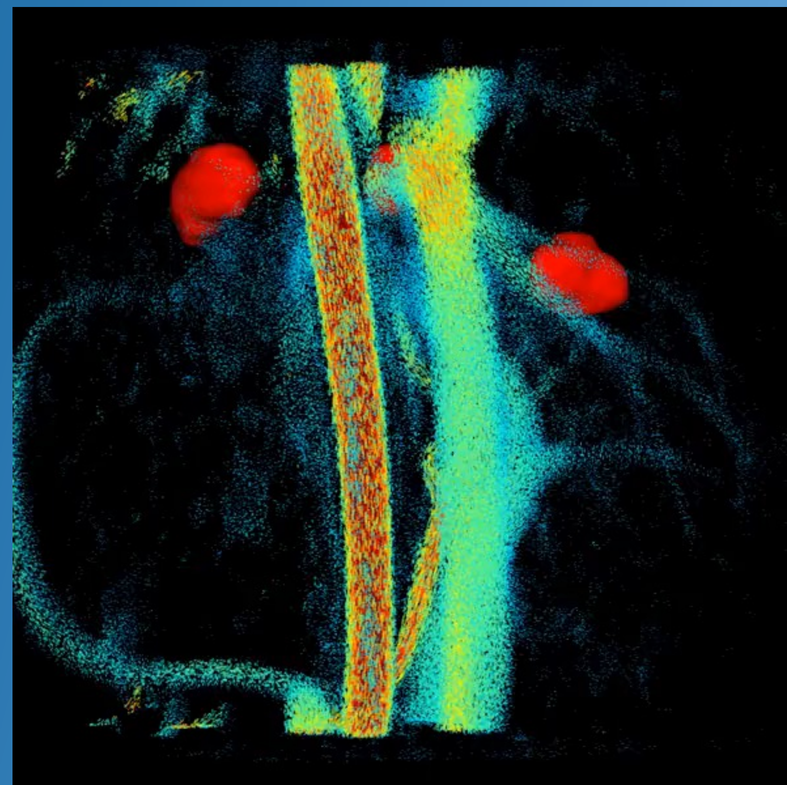

Predicting ablation volume

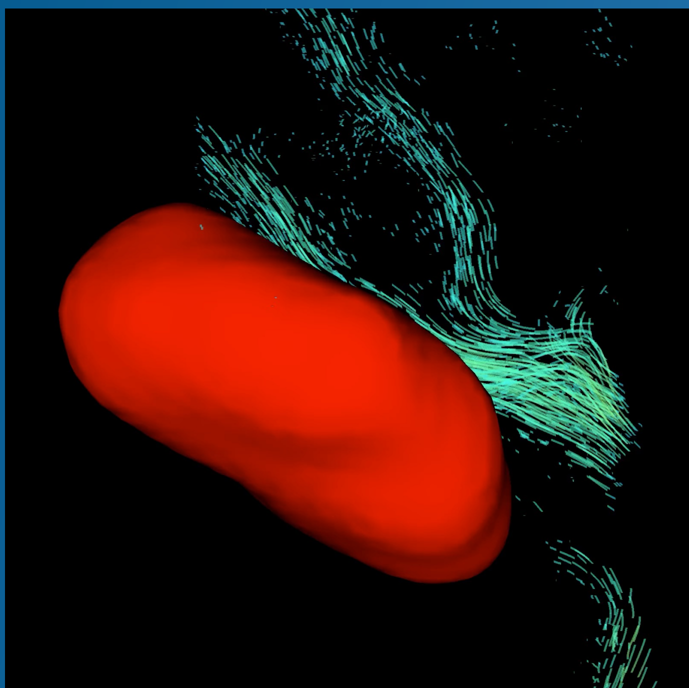

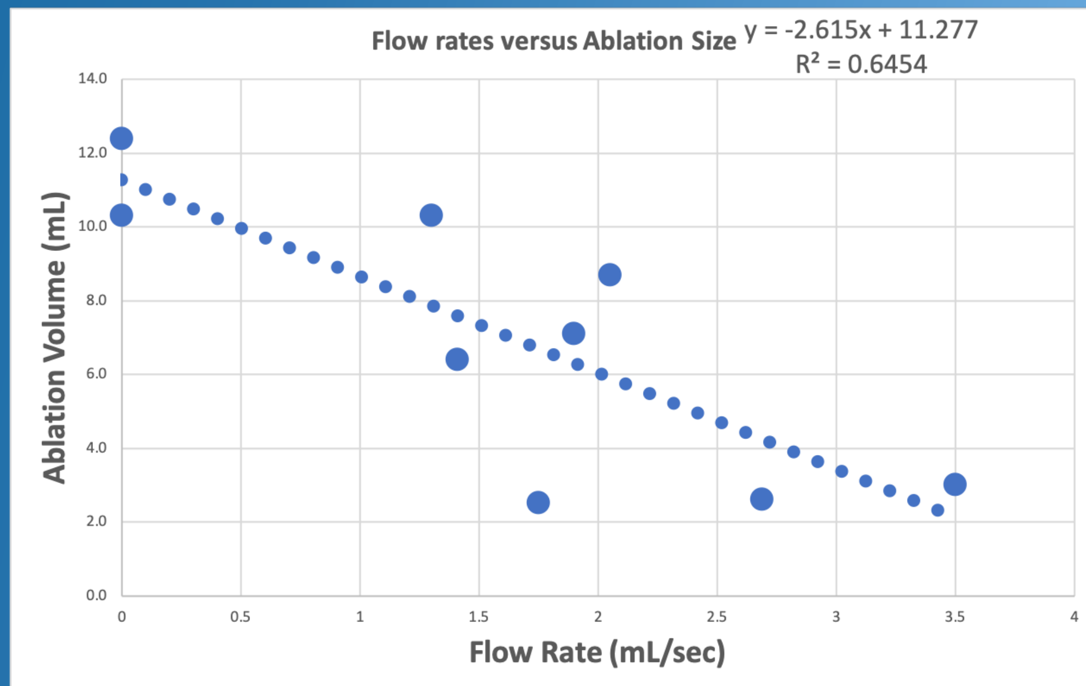

Modeling Heat and Mass Transfer

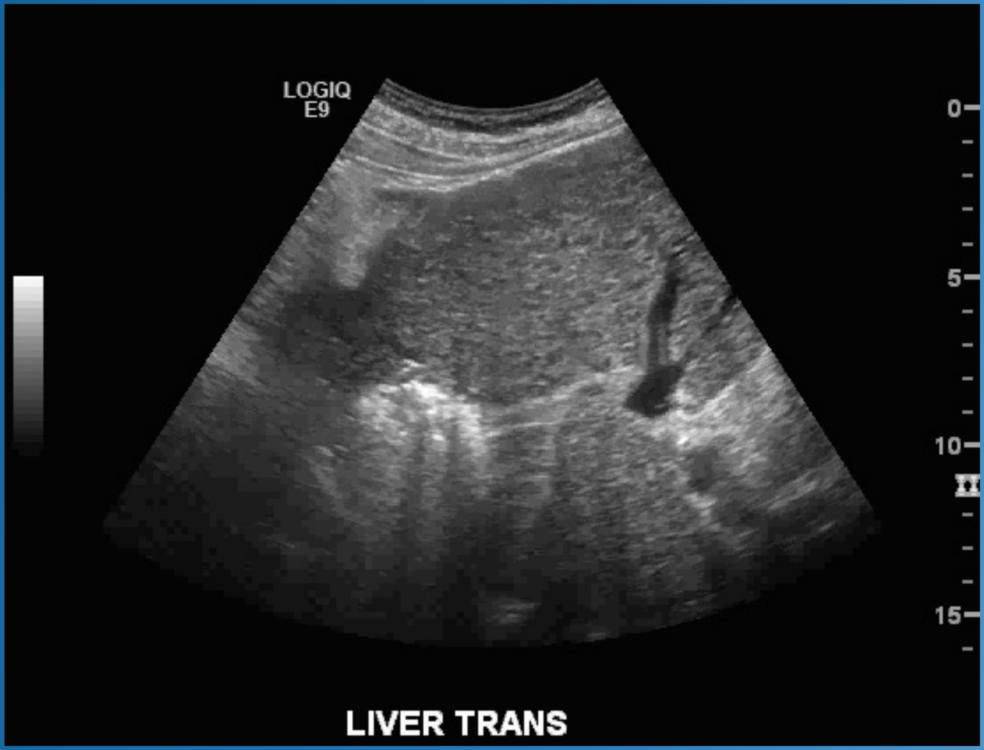

Modeling MWA: Incorporating water vapor

Solve heat transfer equation in porous media

$$(\rho c)_{eq}\frac{\partial T}{\partial t} + \rho_L C_{\rho L}\boldsymbol{u}\cdot\nabla T = \nabla\cdot\left(k_{eq}\nabla T\right) + Q$$

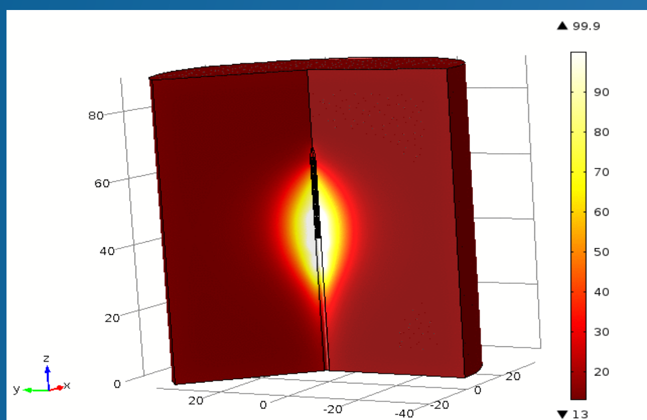

Solve for liquid water and water vapor diffusion through liver tissue

$$\frac{\partial c}{\partial t} + \boldsymbol{u}\cdot\nabla c = \nabla\cdot(D\nabla c) + R$$

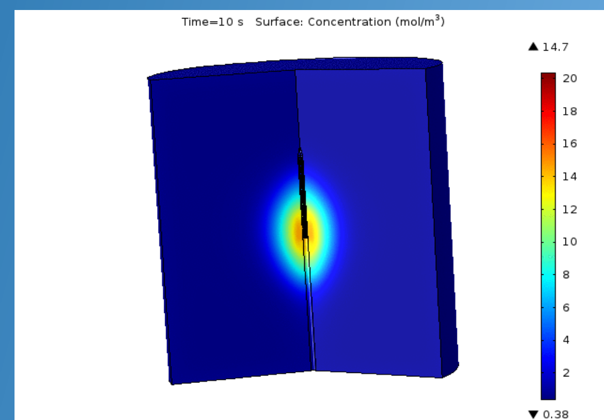

Chiang, Jason, Sohan Birla, Mariajose Bedoya, David Jones, Jeyam Subbiah, and Christopher L. Brace. "Modeling and Validation of Microwave Ablations with Internal Vaporization." *IEEE Transactions on Bio-Medical Engineering* 62, no. 2 (February 2015): 657–63.

Water vapor diffusion = Contraction

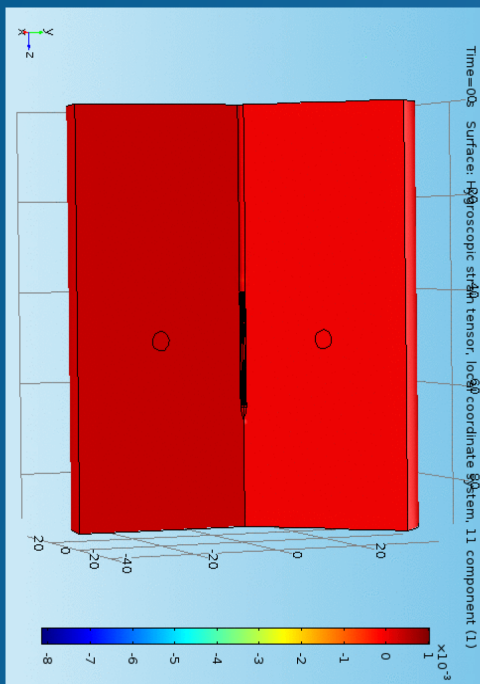

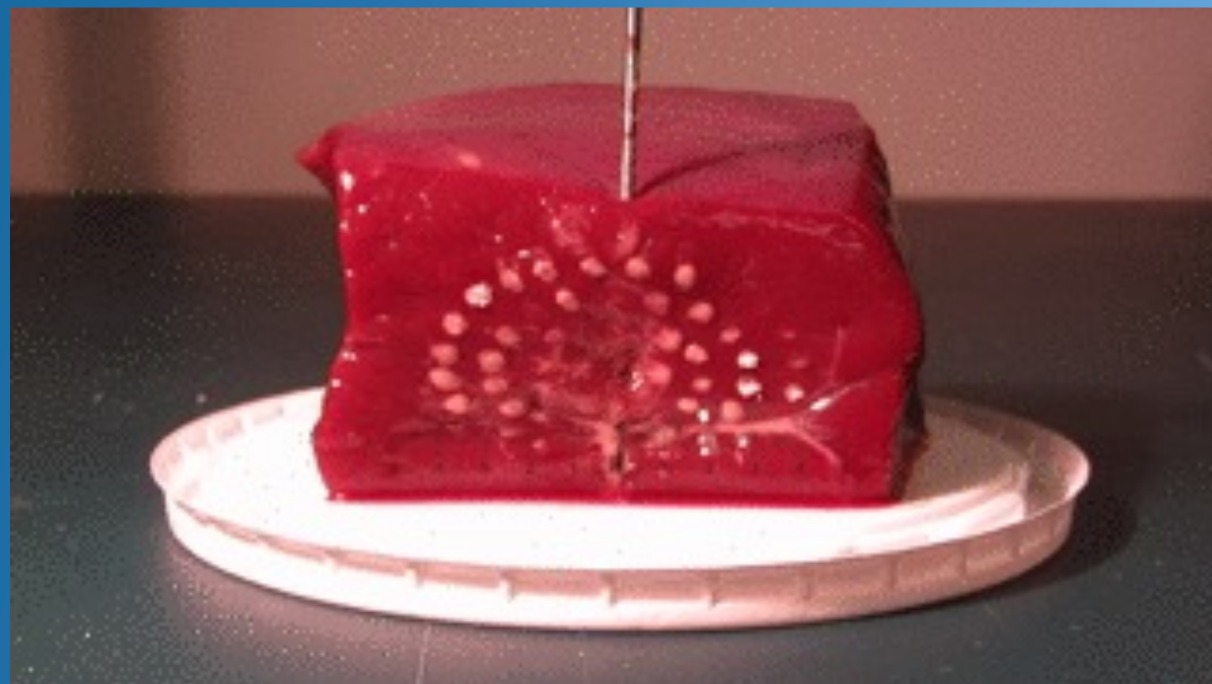

Contraction in Clinical Practice

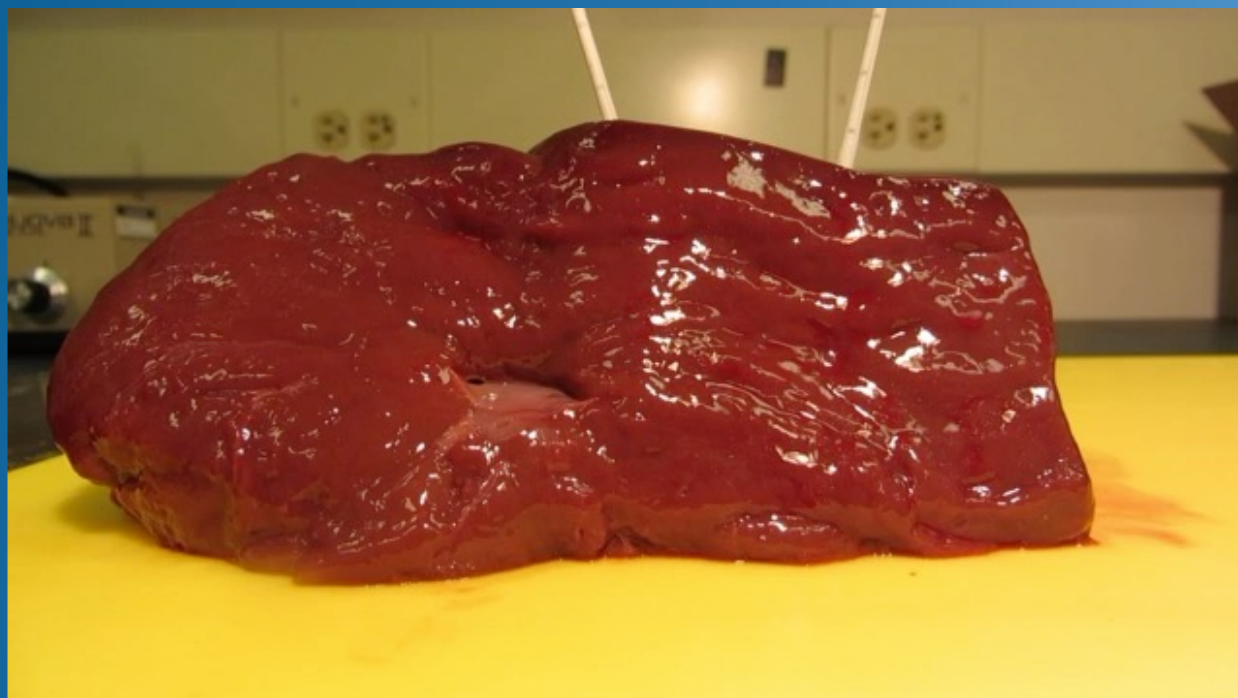

MR thermometry during Thermal Ablation

GOAL: To develop a PRF-based MR thermometry technique for monitoring temperature during MR-guided Liver Ablation

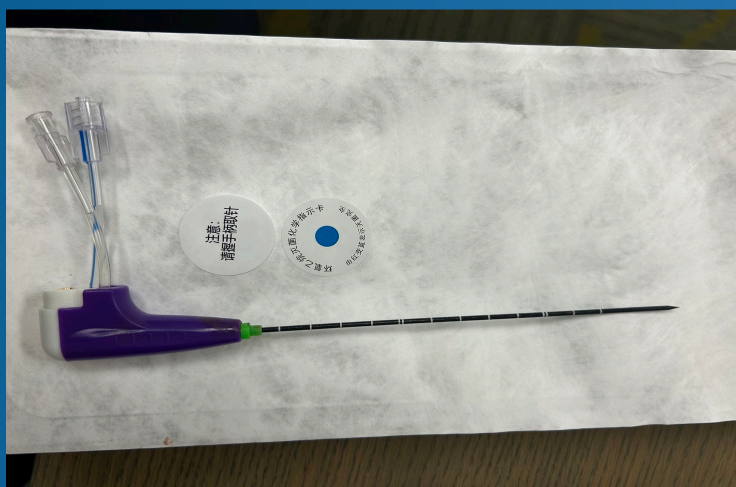

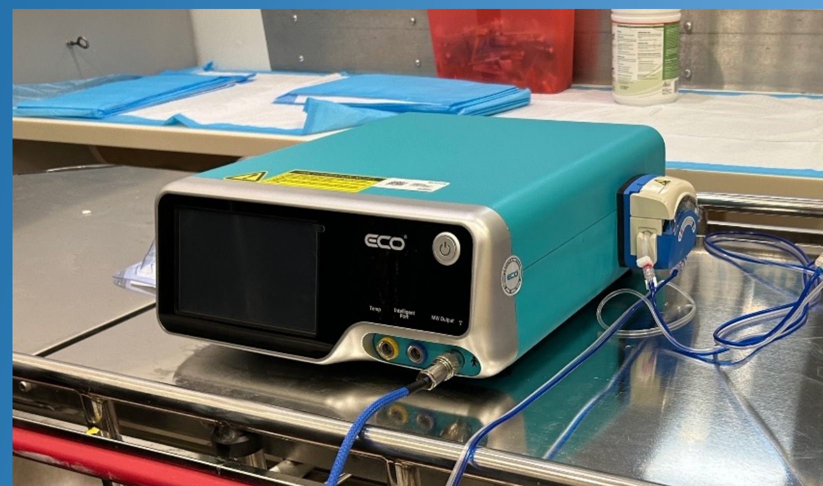

Targeting → Ablation → Evaluation

In-vivo visualization and **targeting** of MR-compatible MWA antennas

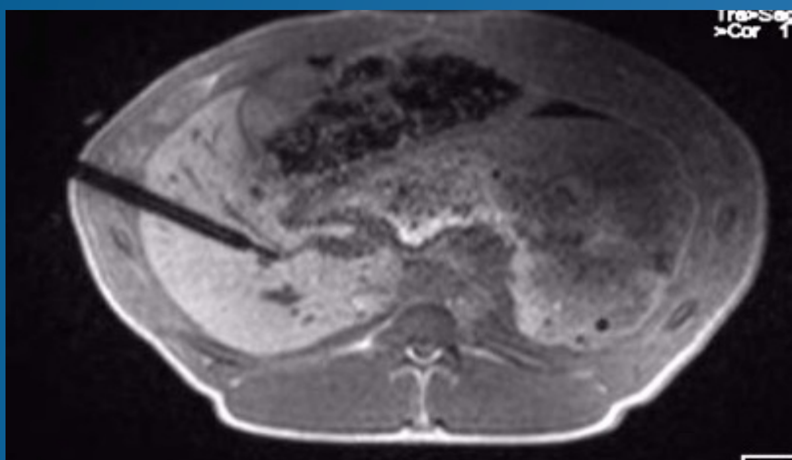

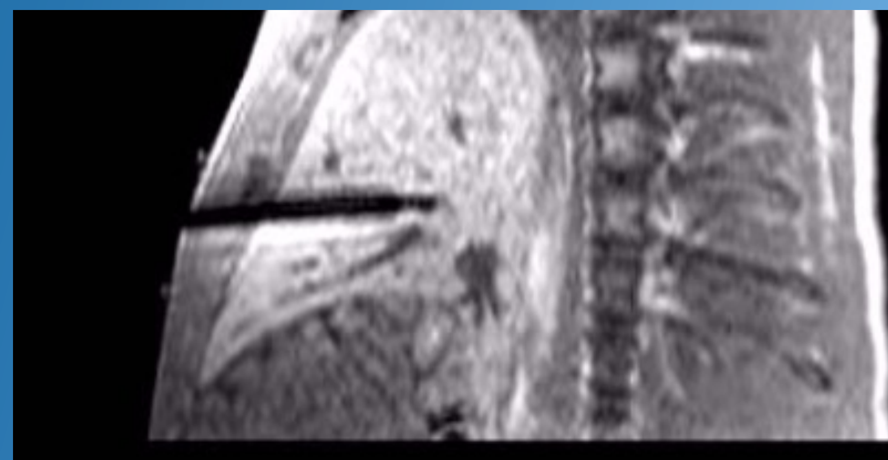

Targeting → **Ablation** → Evaluation

After ablation — Reference

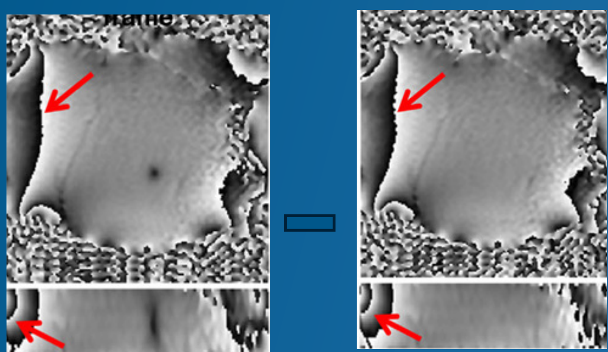

PRF temperature map

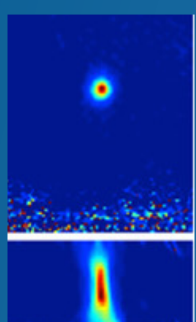

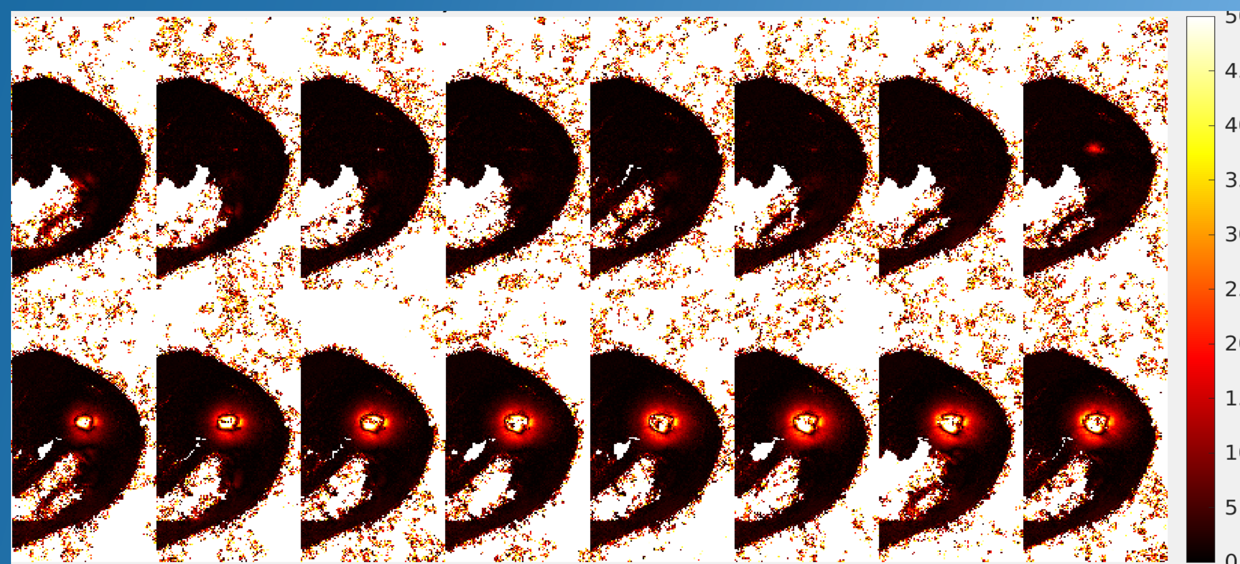

Temperature map after phase unwrapping

Targeting → Ablation → **Evaluation**

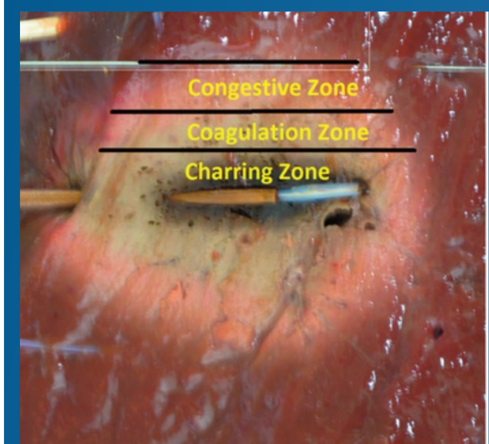

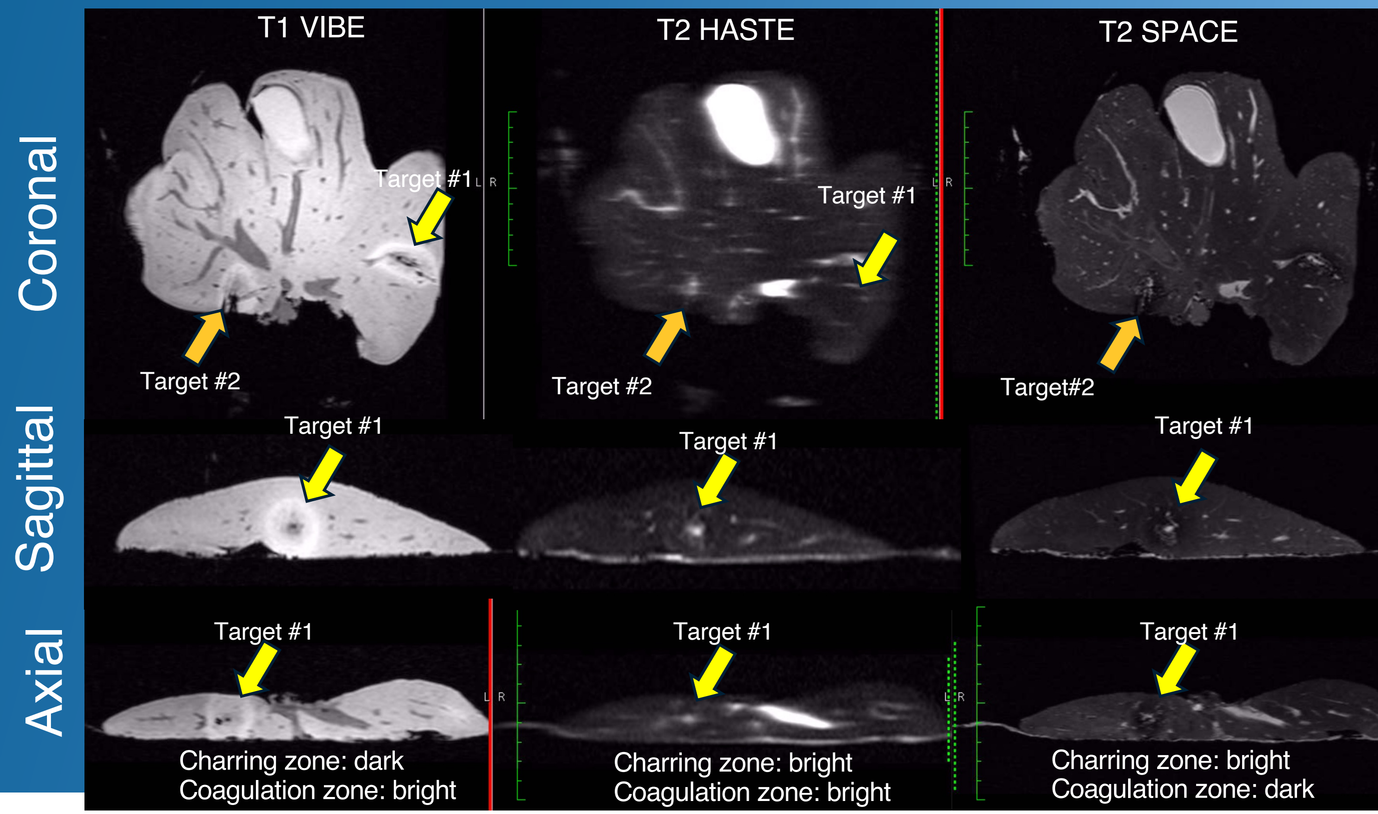

MR Thermometry Near Critical Structures

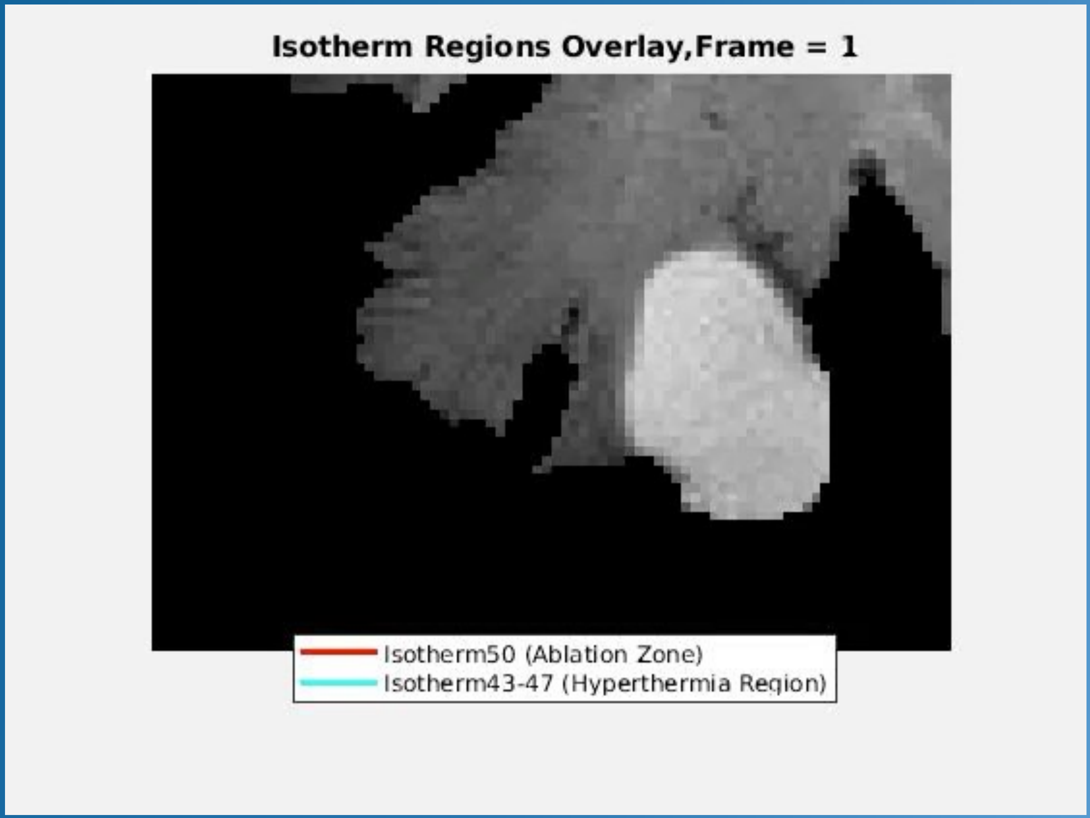

Current state of microwave planning and modeling

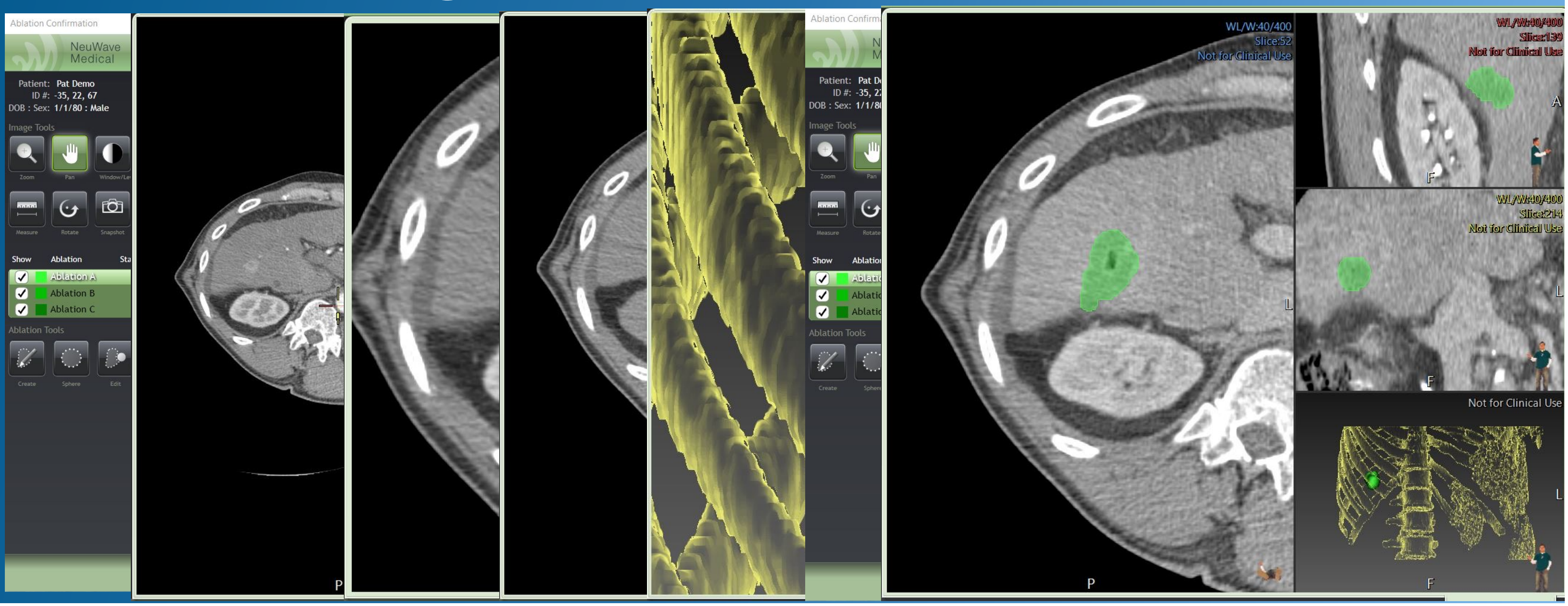

Integrating contraction into MWA planning

20%

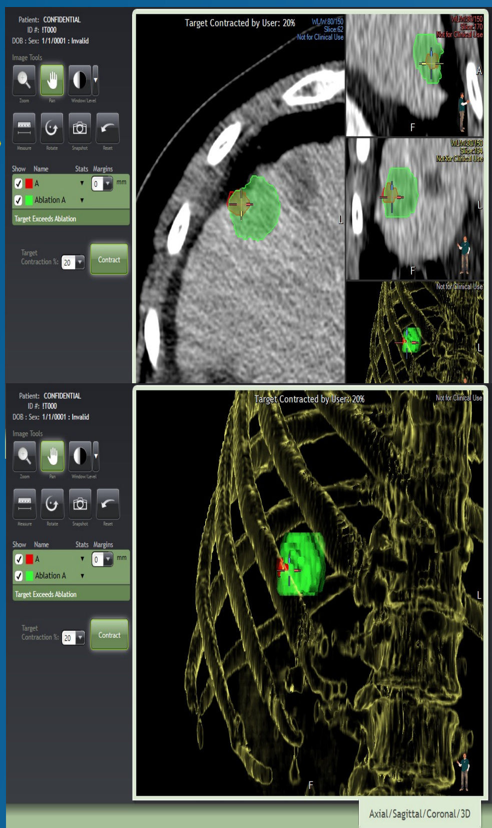

30%

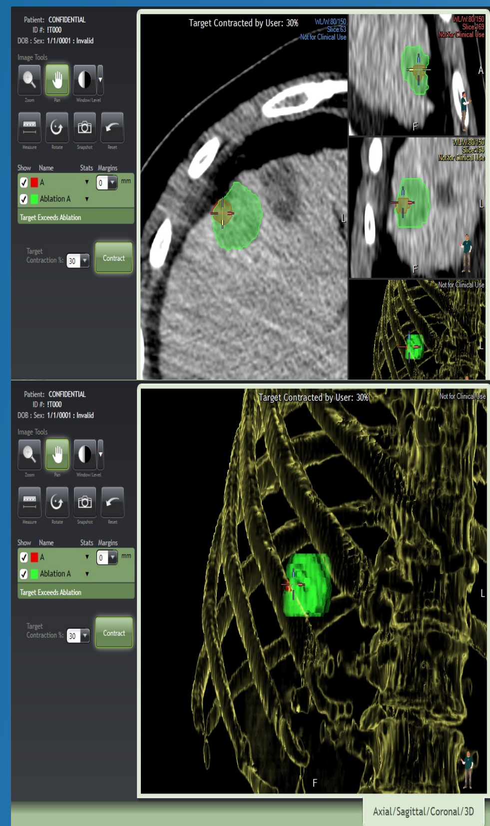

40%

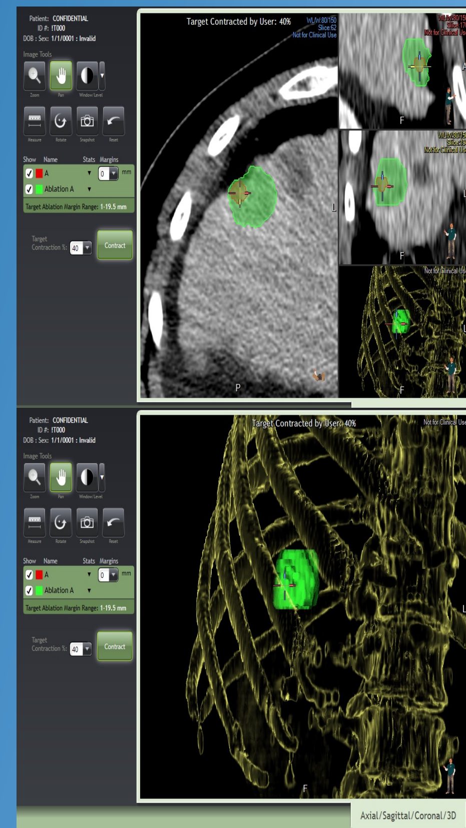

Back to original case: Diagnostic evaluation

8/27

10/15

Transarterial chemoembolization + ablation

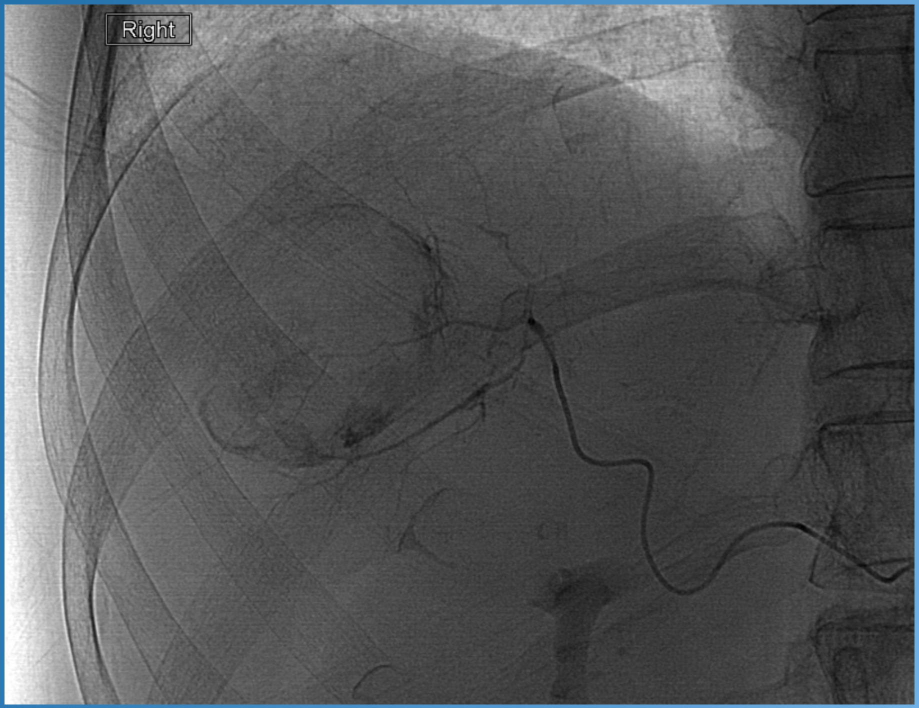

Post-embolization **ablation**

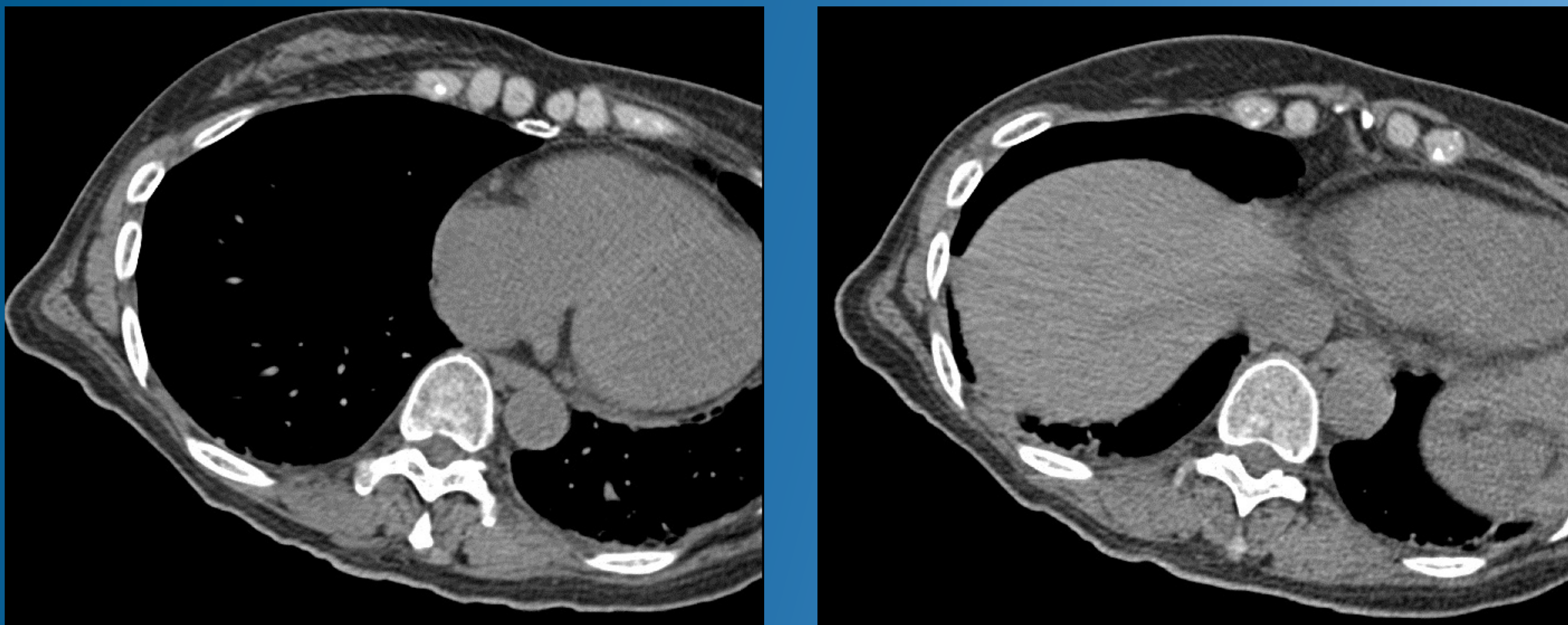

Post-ablation CT scan

Perfusion MRI

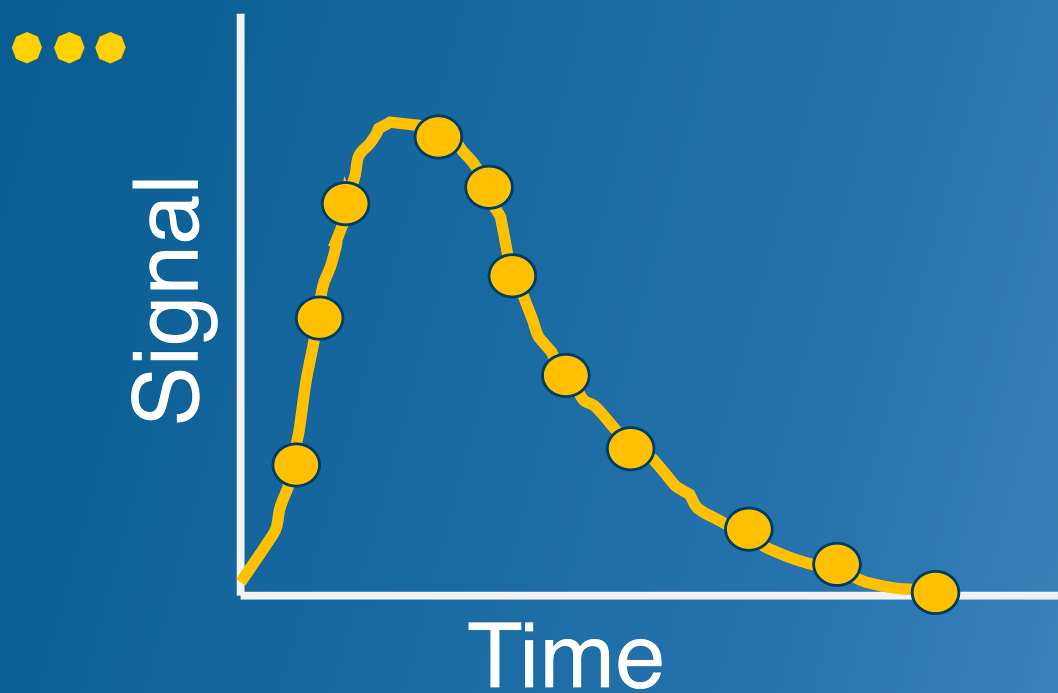

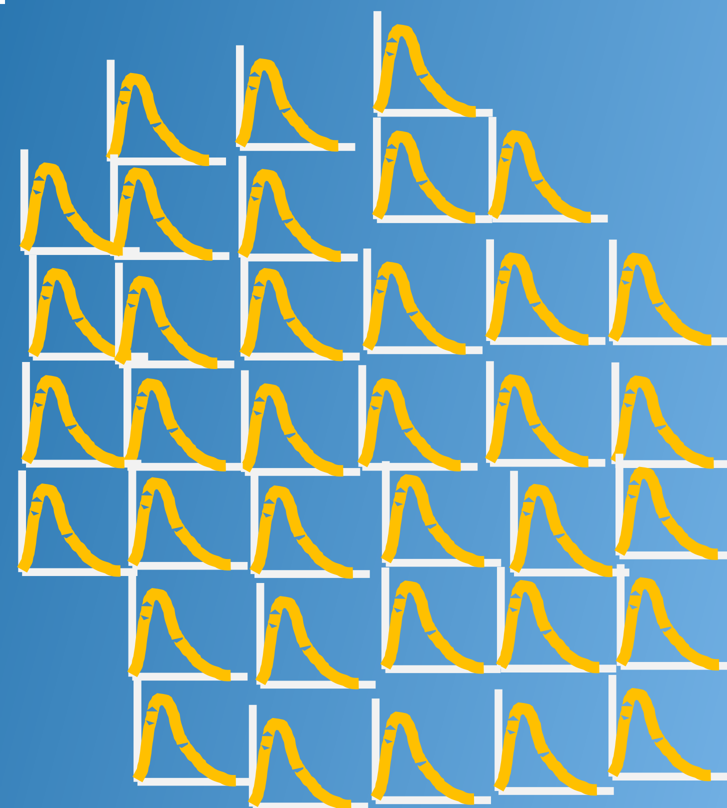

Standard contrast-enhanced MRI vs DCE-MRI

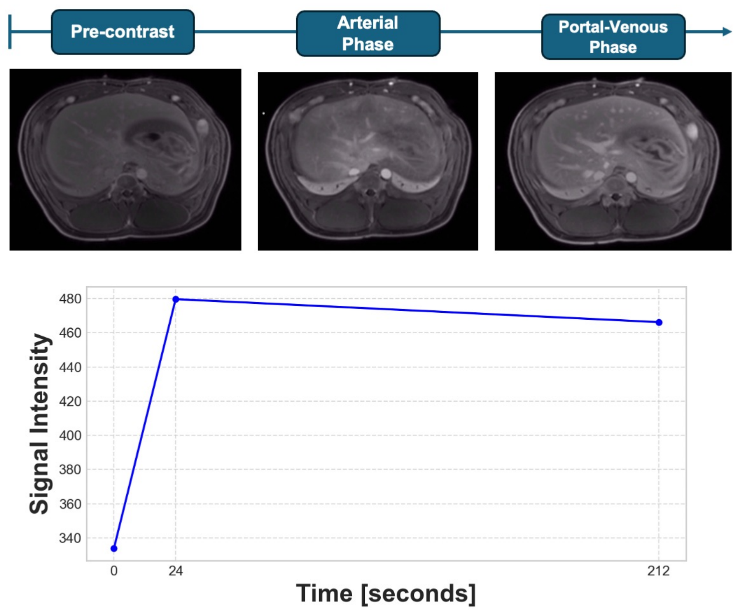

Conventional Multi-Phase Contrast-Enhanced MRI (CE-MRI)

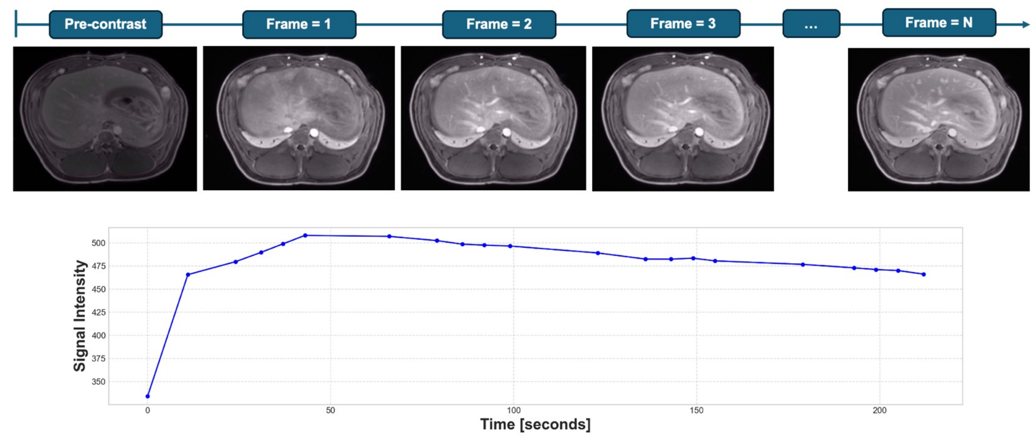

Dynamic Contrast-Enhanced MRI (DCE-MRI) for Quantitative Analysis

Modeling Perfusion with Tofts model

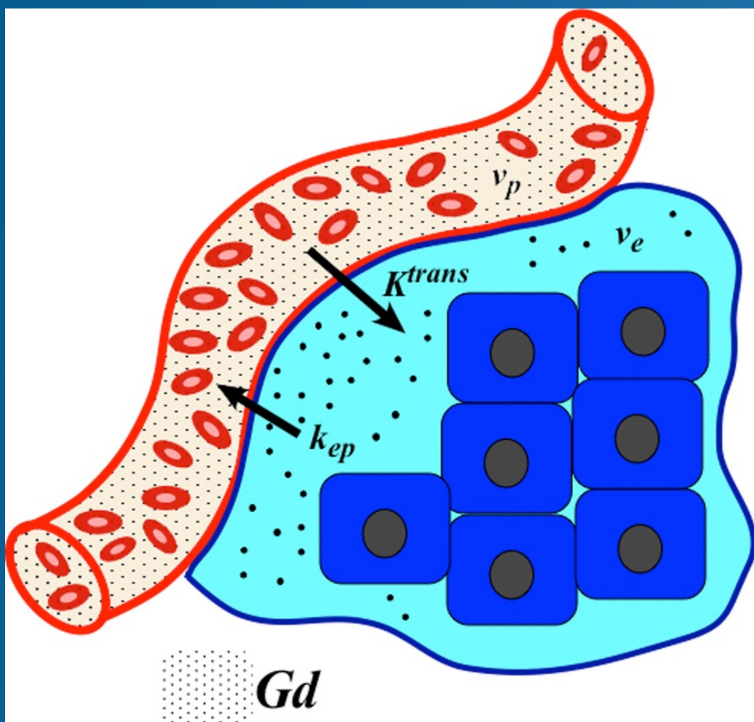

$$C_t(t) = v_p C_p(t) + K^{trans} \int_0^t C_p(\tau) e^{-(K^{trans}/v_e)(t-\tau)} d\tau$$

- $C_t(\tau)$ is the total tissue contrast agent concentration
- $C_p(t)$ is the time-varying blood plasma concentration after a bolus of gadolinium is administered
- K_{trans} (min_{-1}) is the forward rate constant
- k_{ep} (min_{-1}) is the backward rate constant.

Calculating free parameters Ktrans and kep required an assumption of the arterial plasma concentration Cp(t), for which a population-derived arterial input function

Pre-/Post-embolization perfusion curves

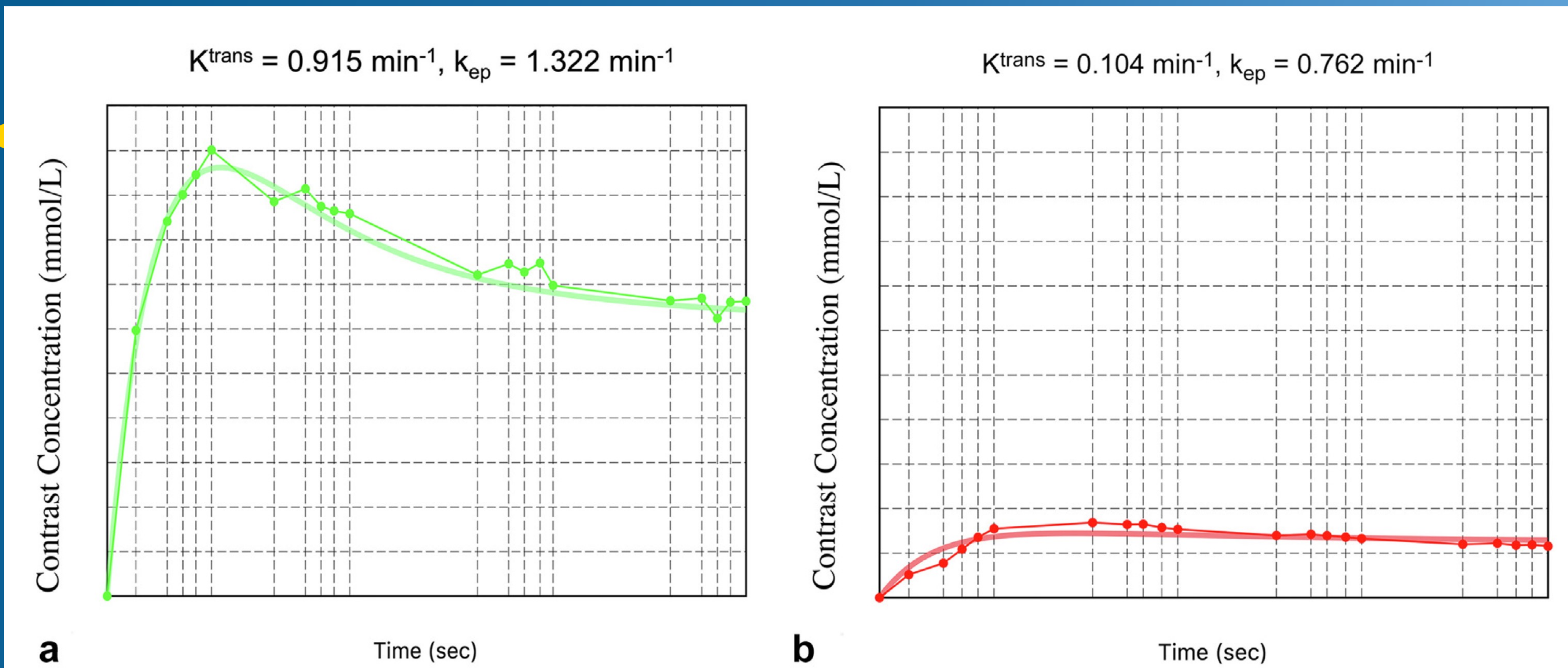

Study Question

Can pre-ablation perfusion MRI predict the microwave ablation zone sizes near liver vessels in an in-vivo liver model?

In Vivo Study Design

Treatment-naïve pigs (n=5) → Hepatic Embolization → Microwave Ablation → Ablation zone volume measurements

Treatment-naïve pigs → DCE Imaging

Hepatic Embolization → DCE Imaging

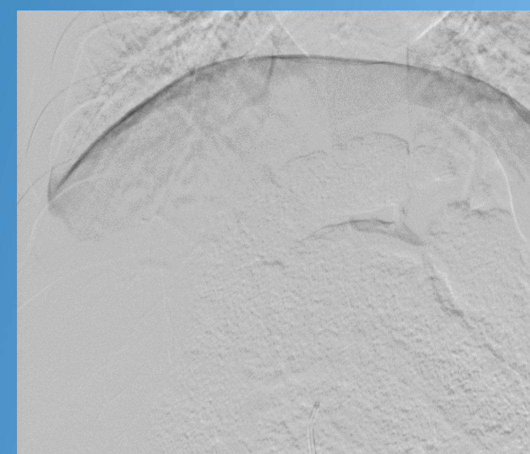

Study goal:
Correlation of post-embolization perfusion with ablation volume in combination therapy

Modeling the effects of perfusion

Heat source

$$\nabla \cdot k\nabla T - \rho_b c_b \omega_b (T_{a0} - T) + q_m + Q = \rho c \frac{\partial T}{\partial t}$$

Thermal conduction

Blood flow

Metabolic heat

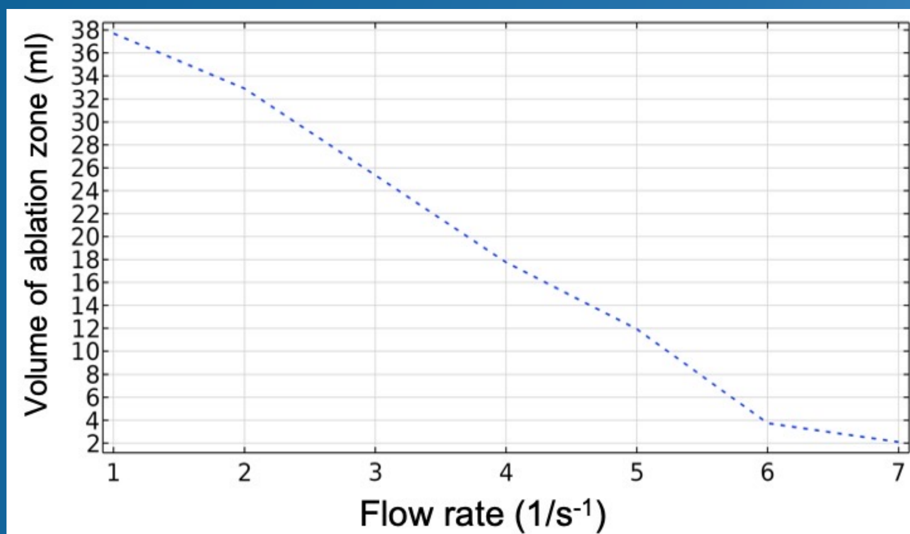

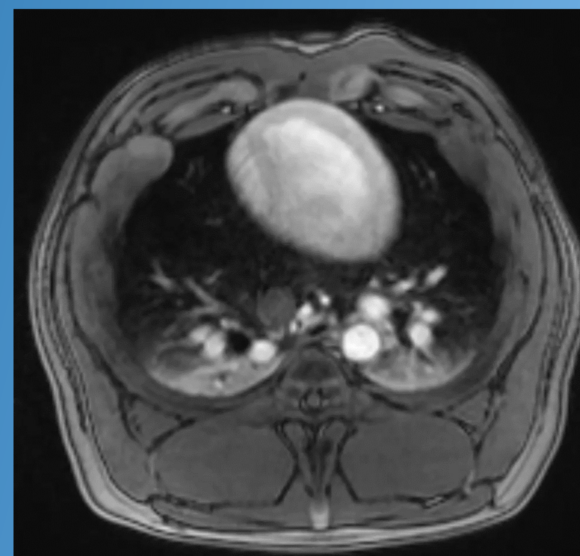

Histopathology and modeling

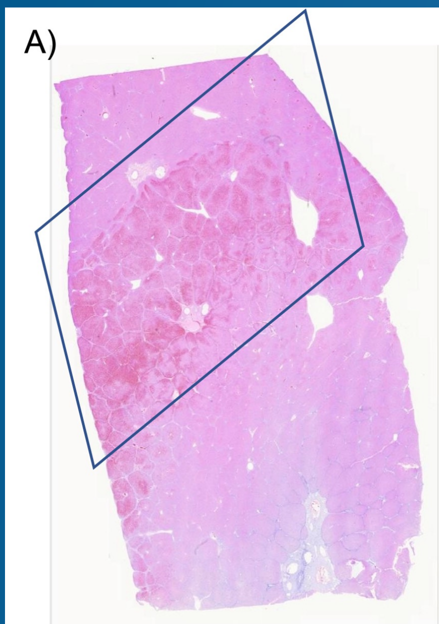

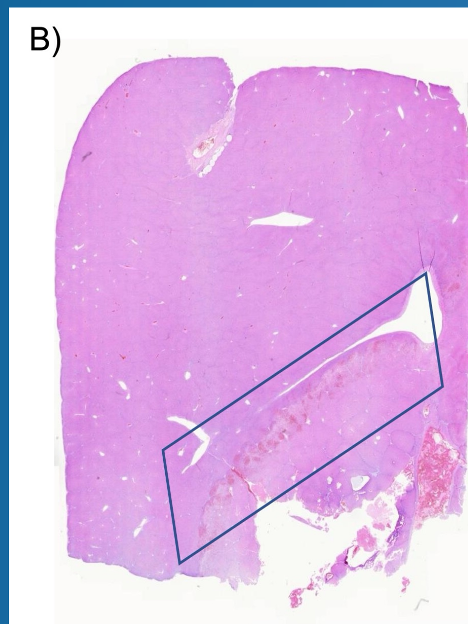

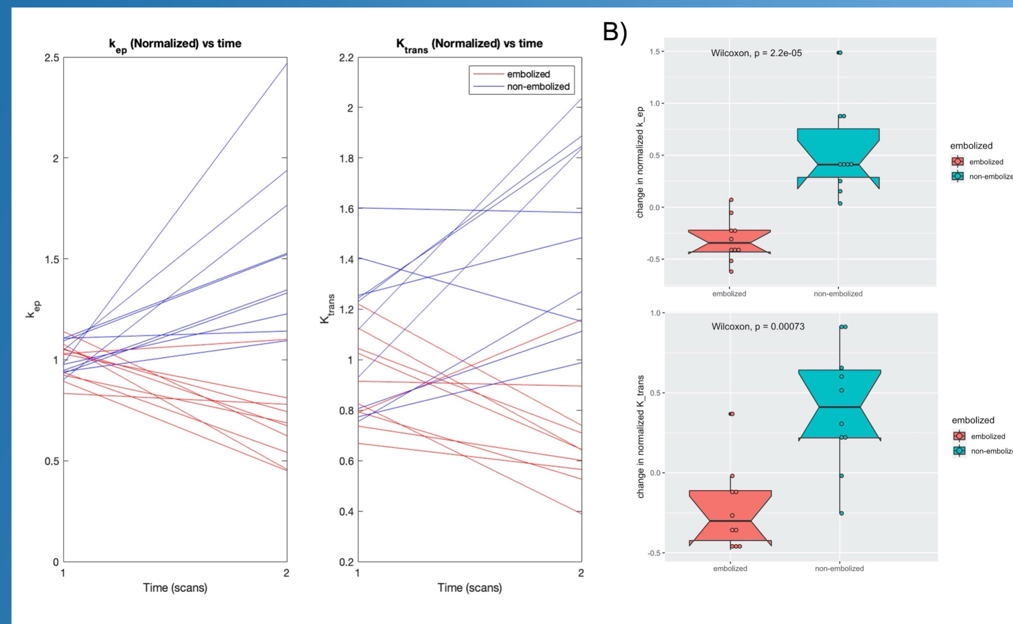

Chiang J, Sparks H, Rink JS, Meloni MF, Hao F, Sung KH, Lee EW. Dynamic Contrast-Enhanced MR Imaging Evaluation of Perfusional Changes and Ablation Zone Size after Combination Embolization and Ablation Therapy. J Vasc Interv Radiol. 2023 Feb;34(2):253-260. doi: 10.1016/j.jvir.2022.10.041.

Correlating DCE-MRI parameters with ablation volume

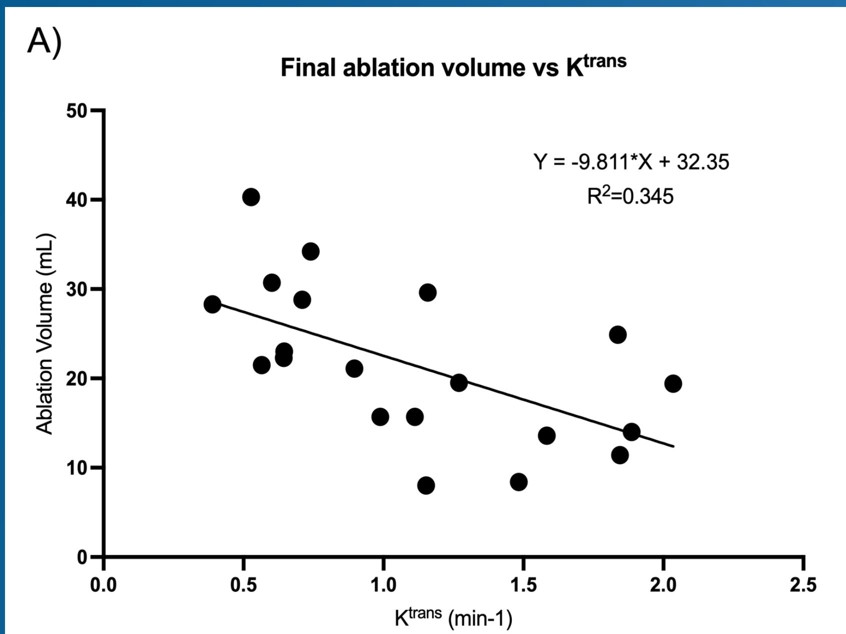

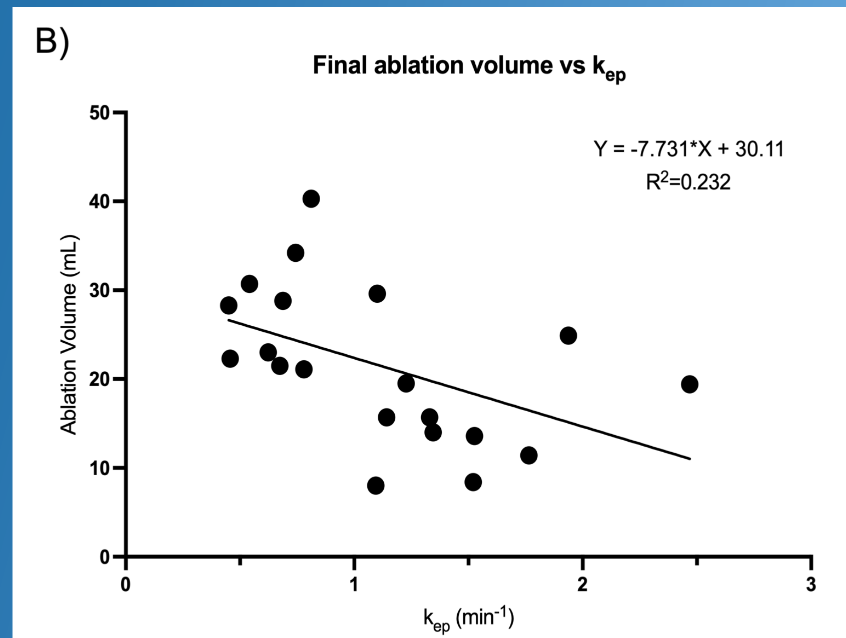

Chiang J, Sparks H, Rink JS, Meloni MF, Hao F, Sung KH, Lee EW. Dynamic Contrast-Enhanced MR Imaging Evaluation of Perfusional Changes and Ablation Zone Size after Combination Embolization and Ablation Therapy. J Vasc Interv Radiol. 2023 Feb;34(2):253-260. doi: 10.1016/j.jvir.2022.10.041.

Validation of numerical models

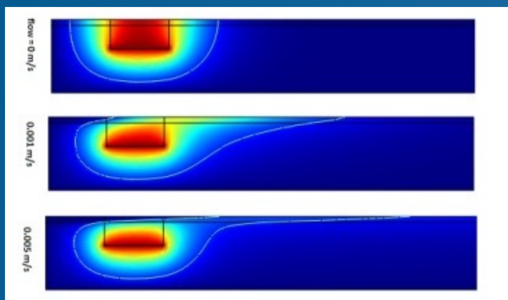

Increasingly complicated numerical models

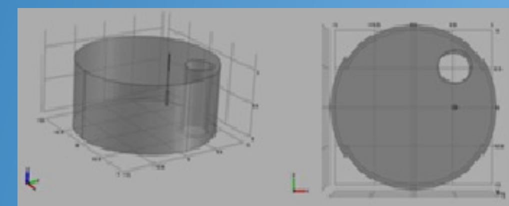

Model Validation

Phantom models

Ex vivo tissue models

In vivo tissue models

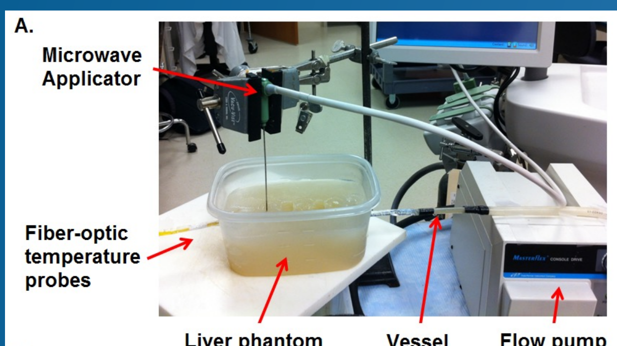

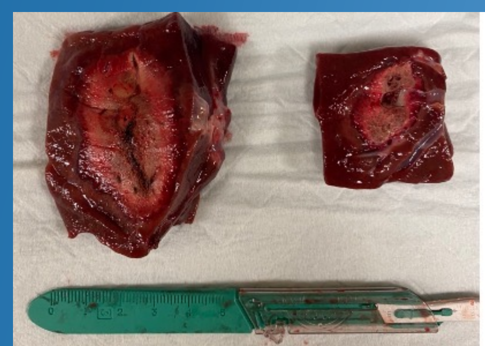

Summary: MR guided interventions

- **Modeling of microwave ablations can more accurately characterize the impact of energy delivery strategies in a complex biological environment.**
  - Patient-specific MR-derived parameters (vascular anatomy, tissue properties, water vapor movement, contraction) Give physicians a tool to predict when more aggressive needle placement or power settings are warranted.
  - Repeat in silico instead of in patient.

- **Validation is critical to any model – large animal model studies required to truly move the needle forward**

Acknowledgements

- **Dept of Radiology**
- David S.K. Lu, MD
- Steven S Raman, MD
- Edward W. Lee, MD, PhD
- Justin McWilliams, MD
- Holden Wu, PhD
- Kyung Sung, PhD

RSNA R&E FOUNDATION

UCLA Health | Jonsson Comprehensive Cancer Center

NIH National Institute of Biomedical Imaging and Bioengineering | Technologies to Shape the Future of Health

Thank You